



# Method for estimating parameters of practical ship manoeuvring models based on the combination of RANSE computations and System Identification



M. Bonci<sup>a</sup>, M. Viviani<sup>a,\*</sup>, R. Broglia<sup>b</sup>, G. Dubbioso<sup>b</sup>

<sup>a</sup> DITEN – Naval Architecture and Marine Engineering Group, University of Genoa, Via Montallegro 1, 16145 Genova, Italy

<sup>b</sup> CNR-INSEAN, National Research Council-Marine, Technology Research Institute, Via di Vallerano 139, 00128 Rome, Italy

## ARTICLE INFO

### Article history:

Received 14 August 2014

Received in revised form 9 June 2015

Accepted 10 June 2015

Available online 17 July 2015

### Keywords:

System Identification

Manoeuvrability

Computational Fluid Dynamics

System based manoeuvrability models

## ABSTRACT

In this work a method for estimating parameters of practical ship manoeuvring models based on the combination of RANSE computations and System Identification procedure is investigated, considering as test case a rather slender twin screw and two rudders ship. The approach consists in the estimation of the hydrodynamic coefficients applying System Identification to a set of free running manoeuvres obtained from an in-house unsteady RANS equations solver, which substitute the usually adopted experimental tests at model or full scale. In this alternative procedure the numerical quasi-trials (in terms of kinematic parameters time histories and, if needed, forces time histories) are used as input for the System Identification procedure; the aim of this approach is to reduce external disturbances that, if not properly considered in the mathematical model, may compromise the identification results, or at least amplify the well-known “cancellation effects”. Furthermore, the CFD results provide information both in terms of flow field variables and hydrodynamic forces on the manoeuvring ship. These data may be adopted for a better understanding of the complex flow during manoeuvres, especially at stern, providing also additional information about the interaction between the various appendages (including rudders) and the hull. The identification procedure is based on an off-line genetic algorithm used for minimizing the discrepancy between the reference manoeuvres from CFD and those simulated with the system based modular model. The discrepancy was measured considering different metric functions and simplified formulations which consider only the main macroscopic parameters of the manoeuvre; the metrics have been analyzed in terms of their capability in reproducing the time histories and in limiting the cancellation effect of the hydrodynamic derivatives.

© 2015 Elsevier Ltd. All rights reserved.

## 1. Introduction

System Identification (SI) has been widely applied in the last decades in several research studies such as the well-known works of Hwang and Abkowitz with the application of Extended Kalman Filter (EKF) [1,2] and recursive maximum likelihood estimation [3], including also the fourth degree of freedom (roll) [4]; more recently, the application of different manoeuvres for the improvement of identification results was proposed [5,6]; Yoon and Rhee proposed the Estimation Before Modeling (EBM) technique [7], while Bhattacharyya proposed a method for System Identification in frequency domain [8] and Zou proposed the application of support vector machines (SVM), both for 3 DOF [9] and 4 DOF models [10].

In [11,12] a procedure based on the offline application of genetic algorithms was proposed. This procedure was systematically applied [13] to a series of ships of the same type (namely fast twin screw ships) and the analysis allowed to obtain ad hoc corrections to existing regression formulas for ship manoeuvrability hydrodynamic coefficients. On one hand, this methodology has been demonstrated to be a valid alternative to cheaply derive the hydrodynamic coefficients that describe the manoeuvring qualities of a marine vehicle and, on the other hand, to identify the mathematical representation that better fits with free running experimental manoeuvres.

When compared with other methodologies employed in marine context, i.e. experimental tests and direct numerical predictions by CFD, System Identification (SI) shows a good level of accuracy, requiring limited computational resources. The advantage of SI is that a suitable set of hydrodynamic coefficients can be evaluated by a few free-running trials (usually Turning Circle and ZigZag manoeuvres), as opposed to expensive and time consuming captive model tests by means of the Planar Motion Mechanism (PMM)

\* Corresponding author at: Via Montallegro 1, 16148 Genova, Italy.  
Tel.: +39 0103532547; fax: +39 0103532127.

E-mail address: [viviani@dinav.unige.it](mailto:viviani@dinav.unige.it) (M. Viviani).

or the Rotating Arm (or the analogous CFD calculations). Since the first systematic studies of the ship manoeuvring problem in the late 1960, considerable research effort was dedicated to apply SI techniques in order to synthesize a large number of experimental data, both at full and model scale [2]. Moreover, SI potentially represents the most conceivable approach to evaluate the nature of the scale effects affecting ship manoeuvrability, if successfully adopted on manoeuvres at model and full scale.

In recent years Computational Fluid Dynamics (CFD) techniques were successfully applied to different problems in the context of ship hydrodynamics, in particular for the prediction of resistance and propulsive performance. With the increase of computational and memory storage capabilities of modern computers, the simulation of off-design aspects related to the ship operations proliferated. In particular, the simulation of the manoeuvring capabilities of a ship has considerably improved during years, as demonstrated by the results reported in the Proceedings of SIMMAN 2008 and 2014 [14,15]. CFD tools allow to analyze complex hydrodynamic features that are difficult (and expensive) to inspect via flow visualization techniques and which are usually not included in the simplified system based modular models adopted for ship manoeuvrability simulations. Moreover, from the integration of the normal and tangential stresses, the forces and moments acting on the hull and its components (appendages and control surfaces) can be directly quantified. This represents a further advantage with respect to experimental techniques, where a direct measurement of the separated forces may be extremely challenging and time consuming. Especially in the case of twin screw ships, which are usually characterized by a rather “rich” appendages configuration, the modular approach (promoted by the MMG group), in which captive model tests are carried out with the hull removed by one or more of its components, is hardly applicable. This approach, though very effective, may not be applied routinely for complex configurations of appendages, because of the high number of expensive and time consuming model tests.

On this basis, CFD simulations of free running model tests result very attractive in the context of System Identification, being able to produce numerical quasi-trials (with kinematic parameters time histories and, if needed, forces time histories), which can be used as input for the System Identification procedure. The quasi-trials results may therefore substitute the more usual model or full scale data. Higher quality data may be obtained from CFD (providing of course the simulations correctness), together with information for improving the physically based modelling of the simplified manoeuvring mathematical models.

In a recent work [16] the effectiveness of the use of free running tests simulated by CFD in SI studies was shown, comparing the outcomes of the identification when using EFD and CFD data. Hydrodynamic coefficients included in a 4 degrees of freedom (DOF) system based model are estimated from only a few CFD free running simulations employing Extended Kalman Filtering (EKF) and Constrained Least Square (CLS) System Identification methods. The set of hydrodynamic coefficients analyzed in the study is rather large (about 30 coefficients for the 4DOF model), since the aim was to reproduce at best the manoeuvres of the specific ship considered; actually, results are rather satisfactory, allowing to obtain very good simulations of the ship manoeuvrability not only for the manoeuvres considered in the identification loop, but also for other manoeuvres adopted for validation. Nevertheless, due to the large number of coefficients contemporarily considered, cancellation effects between the various coefficients are likely to be present, leading to values different from experimental ones. Cancellation effect in SI of ship manoeuvrability is a well-known problem, as shown in many previous studies [1,5,6,11]; this is a phenomenon intrinsic to the strong non-linear nature of ship dynamics that causes the inverse problem to be mathematically ill-posed [17].

Cancellation between coefficients, even if not leading to wrong or unstable results, is always a problem; if the interest is focused only on a single ship, an acceptable input–output model can be obtained also with wrong parameters whose errors compensate each other, however the model may behave unexpectedly outside the validation domain.

The problem is even more problematic, and has to be prevented, if the focus is to analyze systematically a certain number of different ships of the same type, with the final aim to obtain various sets of hydrodynamic coefficients to be successively analyzed in order to obtain new regression formulae or at least tendencies, as presented in [13]. This is of particular interest when many experimental data (full scale trials, free running model tests) are available, as for example in shipyards technical offices; the systematic application of SI may provide an added value to those data, allowing to obtain an estimate of the related hydrodynamic coefficients. In this case, cancellation effect may result in a large scatter of the identified coefficients, making difficult any further analysis to obtain a suitable regression. Similar problems may also arise if SI is adopted in order to estimate scale effects.

Having this in mind, the present System Identification study aims to determine a reliable identification method for the evaluation of the manoeuvrability hydrodynamic coefficients, focusing not only on reproducing the reference manoeuvres, but also on reducing as much as possible the cancellation phenomena during the optimization procedure. The test case considered is a twin screw, twin rudder vessel, described in Section 3. The proposed identification method is based on the application of an offline genetic algorithm (described in Section 2.3) used to modify hydrodynamic coefficients values of a system based mathematical model (described in Section 2.2) to reduce discrepancy between simulations and reference values. In this case, reference values are represented by simulations of free running tests obtained with an in-house RANS code (described in Section 2.1). Different tests have been performed (see Section 4.2) considering various optimization objectives, based on the macroscopic characteristics of the manoeuvre as well as on metric functions that evaluate the instantaneous error of the time-dependent histories of the kinematic manoeuvring variables.

As mentioned before, the use of CFD to obtain the quasi-trials which are input for the SI presents one important advantage, which is the possibility to obtain the forces acting on the different elements of the ship. In this case, after a first set of tests considering both hull and rudder related coefficients inside the identification procedure, the manoeuvring mathematical model was constrained by imposing the same rudders and propellers forces and moments directly calculated by CFD. On this basis, the identification process is focused to determine the hull hydrodynamic coefficients, the rudder and propeller terms being implicitly accounted for by the aid of CFD data. This results in a reduction of the number of unknowns to be identified, thus reducing the cancellation effects. It has to be pointed out that the use of the rudder and propeller forces to constrain the mathematical model is realistic also in view of the application of the procedure to experimental data, because both the rudder and propeller forces could be measurable quantities during free running model tests.

As a final step, in order to further investigate the benefits from constraining the mathematical model to identify physically consistent hydrodynamic coefficients, the hull hydrodynamic forces and moments were also included in the objective functions, in addition to the kinematic variables.

## 2. Theoretical background

Before presenting the results of the System Identification activity, it is useful to introduce the different tools adopted. In particular,

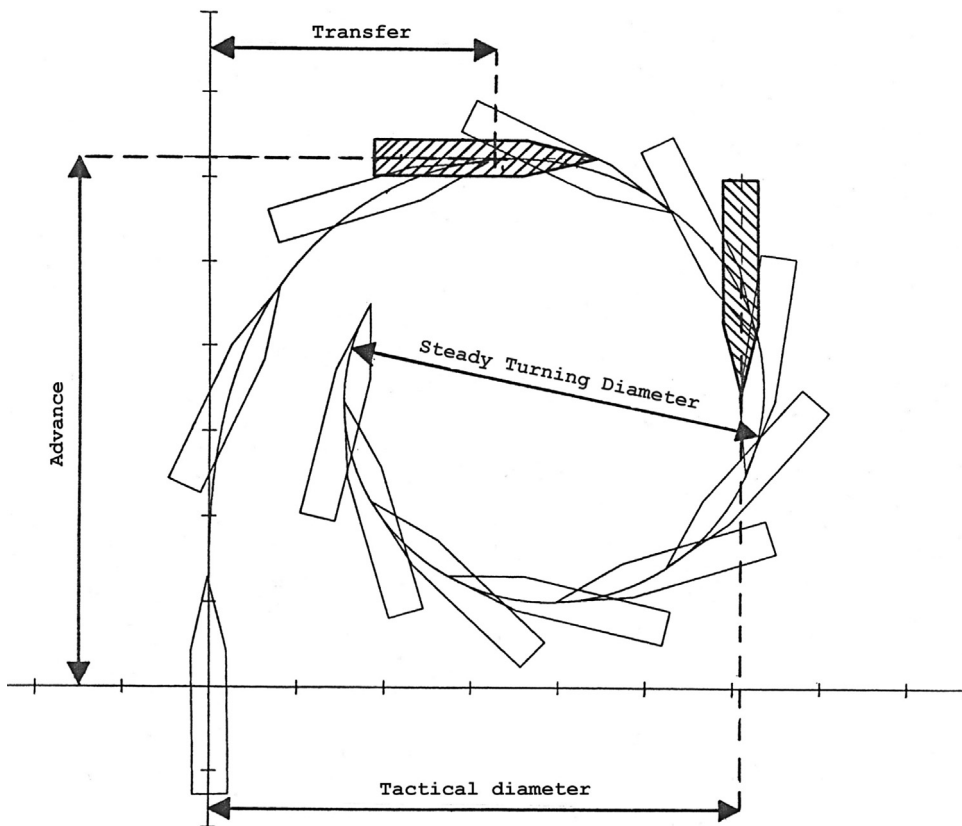


**Fig. 1.** Typical Turning Circle manoeuvre trajectory.

the in-house unsteady RANS solver adopted to produce the free running model tests, used to generate manoeuvrability data which are the base of the System Identification study, is described in Section 2.1; in the same paragraph, a discussion on the accuracy of the CFD tool to reproduce ship manoeuvres is also reported. The system based modular model for manoeuvrability simulations is described in Section 2.2. The coupling between the commercial software modeFRONTIER4, which features the genetic algorithm adopted, and the system based simulator is described in Section 2.3.

Throughout this work, reference is made to Turning Circle and ZigZag manoeuvres. The main parameters considered for the various manoeuvres are defined in the various sections, while in

following Figs. 1 and 2 their main outcomes are reported, showing a typical Turning Circle trajectory and the heading angle and rudder angle time histories for a typical ZigZag manoeuvre respectively.

### 2.1. CFD solver

The CFD code adopted in this study is the solver *xnavis*, which is a general-purpose simulation tool which solves the Navier-Stokes Equations for unsteady high Reynolds number (turbulent) free surface flows around complex geometries. The main features of the solver are summarized here, the interested reader is referred to [18–22]. The solver is based on a finite volume formulation with conservative variables co-located at cell centre. The spatial

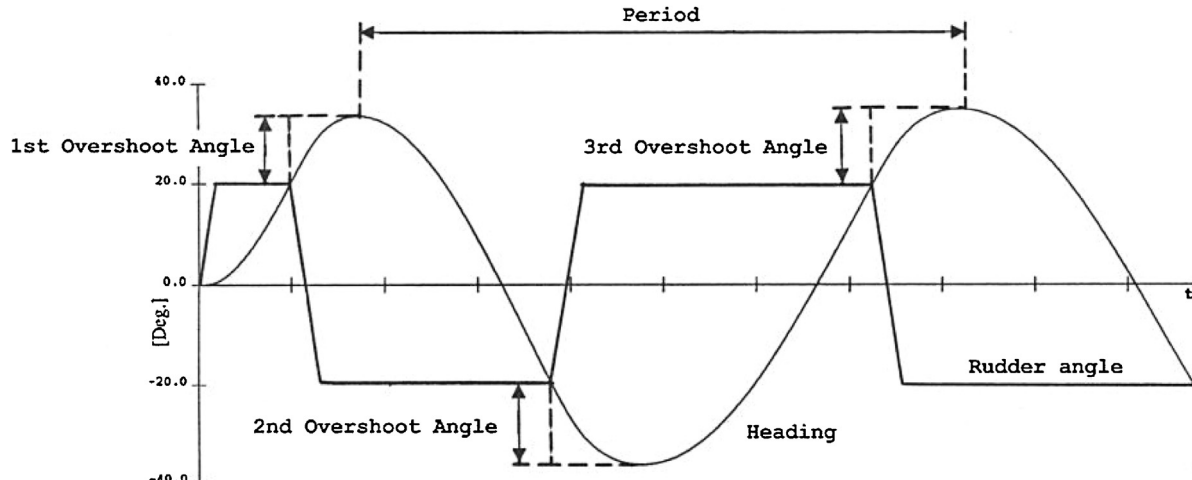


**Fig. 2.** Heading angle and rudder angle time histories for a typical ZigZag manoeuvre.

**Table 1**

Validation on the single rudder configuration.

	EFD		CFD						UA	
	Value	RA	Medium		Fine		RE			
			Value	$\varepsilon\%$	Value	$\varepsilon\%$	Value	$\varepsilon\%$		
Advance	2.85	11.79%	3.22	12.98%	3.02	5.96%	2.95	3.63%	6.62%	
Transfer	1.00	36.32%	1.10	10.00%	1.02	2.00%	0.99	0.67%	7.84%	
Tactical Diameter	2.56	9.82%	2.65	3.48%	2.48	3.13%	2.42	5.33%	6.81%	
Steady Turning Diameter	2.52	1.92%	2.83	12.30%	2.60	3.17%	2.52	0.13%	8.85%	

**Table 2**

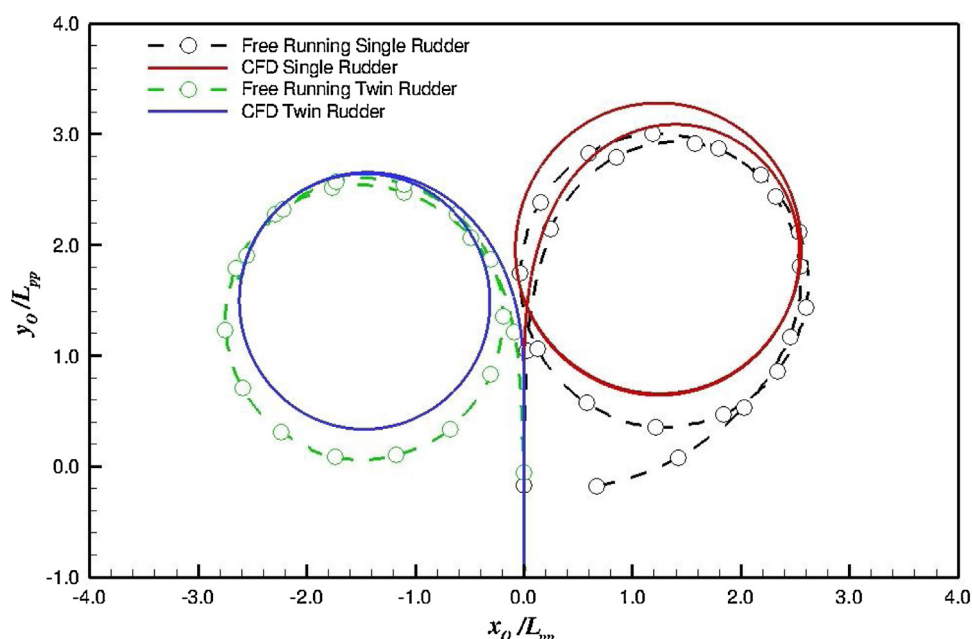
Validation of the twin rudder configuration.

	EFD		CFD						UA	
	Value	RA	Medium		Fine		RE			
			Value	$\varepsilon\%$	Value	$\varepsilon\%$	Value	$\varepsilon\%$		
Advance	2.48	7.54%	2.62	5.77%	2.59	4.44%	2.58	3.99%	1.27%	
Transfer	1.14	6.84%	1.05	7.98%	1.06	7.02%	1.06	6.70%	1.04%	
Tactical Diameter	2.70	3.88%	2.55	5.63%	2.56	5.19%	2.56	5.04%	0.47%	
Steady Turning Diameter	2.55	4.26%	2.18	14.51%	2.31	9.41%	2.35	7.71%	5.63%	

discretization of the convective terms is done with a third order upwind based scheme, whereas the diffusive terms are discretized with second order centred scheme and the time integration is done by second order implicit scheme (three points backward). The divergence free solution at each time step is computed iteratively by a pseudo-time integration that exploits an Euler implicit scheme with approximate factorization, local pseudo time step and multi-grid acceleration [18]. Although several turbulence models have been implemented in the code, in all the simulations reported in present work the turbulent viscosity has been calculated by means of the one-equation model of Spalart and Allmaras [23].

Free surface effects are taken into account by a single phase level-set algorithm [21]. Complex geometries and multiple bodies in relative motion are handled by a dynamical overlapping grid approach [20,24]. High performance computing is achieved by an efficient shared and distributed memory parallelization [22,25].

The propeller effect is simulated by a hybrid actuator disk model. In this model the thrust and torque are evaluated at each time step from the open water curves and are distributed over the propeller disk according to the actuator disk theory [26]. The instantaneous evaluation of the advance coefficient is performed by averaging the axial component of the flow field over the propeller disk. Moreover, in order to estimate the propeller side force that arise in oblique flow conditions, Ribner simplified theory has been implemented in the solver [27]. Further details on this approach are described in [28]. It has to be remarked that, in order to make the use of the open water curves consistent, the self-induction effect is properly accounted for by momentum considerations (axial-symmetric actuator disk theory) [29]. For the sake of completeness, it has to be mentioned that in the Turning Circle simulation the self-induction of the propeller was neglected in present calculations; however, a sensitivity analysis, whose results are reported in [29], has shown

**Fig. 3.** Comparison between the CFD and EFD trajectory for the twin (left) and single (right) rudder configuration.

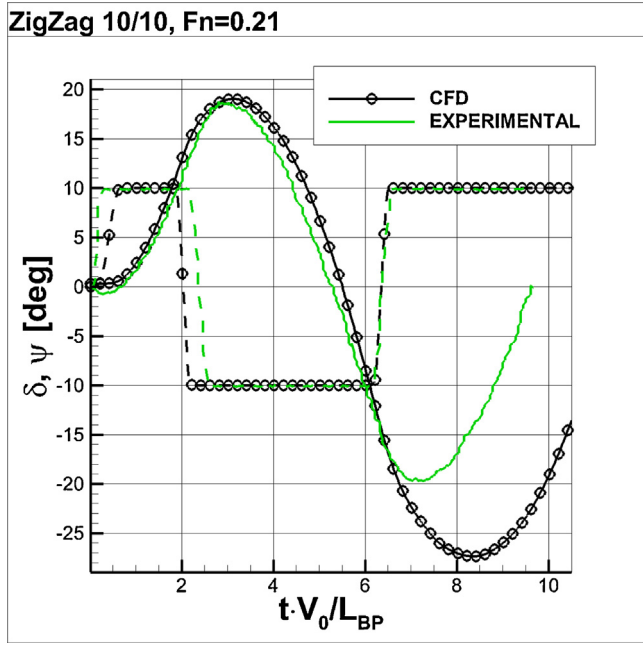


**Fig. 4.** Comparison plot of experimental and numerical free running simulations.

that the effect of the propeller loading conditions is negligible; therefore, the effects of the different propeller model adopted for the two manoeuvres should not affect the outcomes of the System Identification procedures described in the following.

The solver has been widely tested and validated for complex flows around bodies of interest in marine hydrodynamics, such as surface ships, submarines and propellers. In the context of ship manoeuvrability, simulations of both captive (pure oblique flow and oscillatory motion tests) and free running manoeuvres have been carried out. Regarding the captive tests, the solver was validated in terms of manoeuvring forces considering different hull forms; in particular, in [13] the same ship model considered in present work (in single rudder configuration) was investigated, showing a good agreement between numerical and experimental results.

Recent research activities have been dedicated to the prediction of the free running tests of both twin and single screw ships.

In the case of single screw ships, turning circle simulations were carried out on the well-known KVLC2 ship, an extensively studied test case for International CFD Workshops. The simulation of

the 35° Starboard turning circle at a Froude Number equal to 0.143, presented at the last SIMMAN Workshop [30], provided very satisfactory results with respect to the model tests.

In the case of twin screw ships, simulations were carried out [29,31] on the same vessel considered in the present work (see Section 3); two different models of the same ship were considered, having two different stern appendages configurations, namely the one considered in the present work (twin rudder) and an alternative one with a single central rudder. In particular, the single rudder ship was characterized by extremely poor course keeping qualities; this led to a modification of the stern appendages configuration, moving from single rudder to twin rudder configuration and adding a central skeg. Because of the inherent tendency of the bare hull to instability, the manoeuvring prediction by CFD is extremely challenging, especially in the single rudder configuration. The contribution of the stern appendages of the manoeuvring response was assessed, as well as the different behaviour of the rudder-propeller system (related to the rudder-propeller interaction phenomena). The macroscopic parameters of the turning circle manoeuvre of the single and twin rudder configurations are summarized in Tables 1 and 2, respectively, where both numerical and experimental results are reported. In order to verify the numerical results, three grid levels were considered.

Only the results on the medium and fine mesh are reported in the table for the sake of shortness. It has to be stressed that the numerical uncertainty (UA) amounts to 10% (single rudder) and 5% (twin rudder); the average error evaluated considering the extrapolated values, achieved by a Richardson Extrapolation (RE in the table) is about 5% and 10% for the single and twin rudder configuration, respectively. The satisfactory agreement between the numerical and experimental results as well as the differences between the two configurations are further shown, for the sake of completeness, in Fig. 3. For the experimental results, a repeatability analysis was performed considering 5 manoeuvres; the RMS value with respect to the mean value of the different parameters, termed "RA", is reported in the tables; it has to be stressed that the higher values of the repeatability for the transient parameters (Advance and Transfer) in case of the single rudder configuration have to be ascribed to its poorer course keeping characteristics that might have affected the approaching phase before the actuation of the rudder (i.e. non-zero yaw rate and drift angle). The repeatability of the twin rudder configuration is close to that of similar models tested on the same facility.

Despite the satisfactory results obtained for the turning circle manoeuvre, the CFD tool adopted in this study presented larger discrepancies when applied for the simulation of the more unsteady

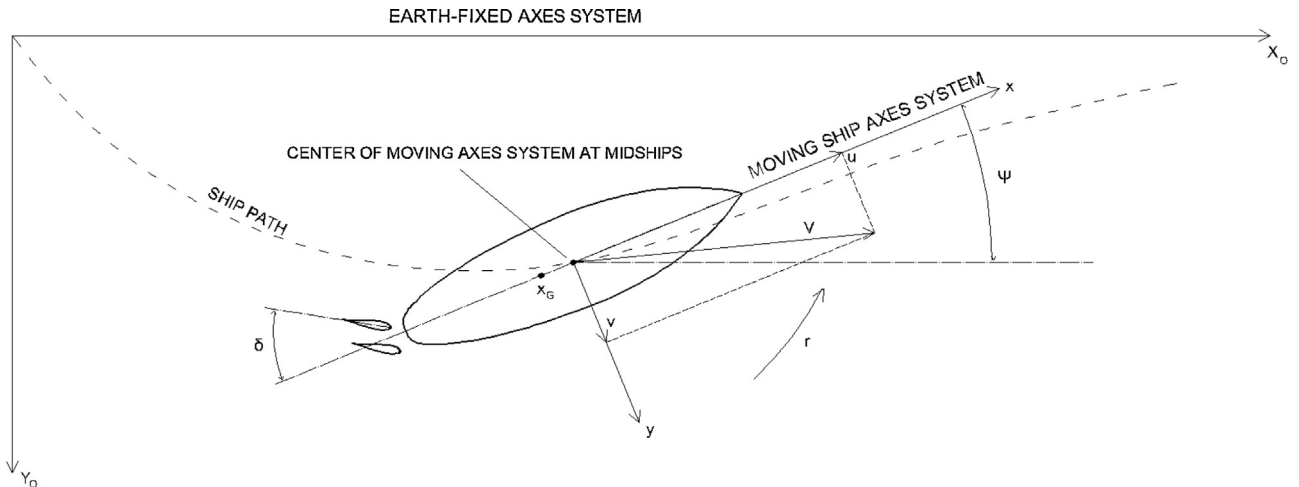


**Fig. 5.** Fixed and moving axes.

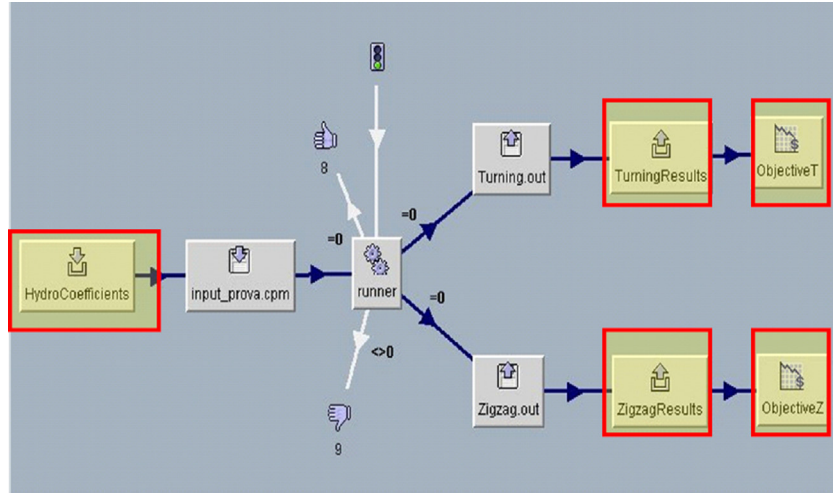


**Fig. 6.** Scheme of the identification process in modeFRONTIER [13].

ZigZag manoeuvre. In particular, Fig. 4 reports the results for the 10°/10° ZigZag manoeuvre in terms of rudder angle and heading for the twin rudder ship model: it is clear that the CFD agrees satisfactorily with the experiments and reproduces the dynamic response of the ship after the first rudder execution up to the 1<sup>st</sup> overshoot angle, whereas the second part of the manoeuvre is poorly captured, being the 2<sup>nd</sup> overshoot angle overestimated by about 40%.

Reasons for this discrepancy are still under examination, and could be ascribed to a not completely satisfactory representation of the propeller forces with the simplified approach proposed. From this point of view, therefore, it is clear that CFD tools, despite being very promising, still need a continuous effort for improvement in order to eliminate issues like this.

Notwithstanding the discrepancies between experimental tests and CFD numerical simulations, in present work the CFD results are considered as the unique reference for System Identification. This choice is in line with the main aim of this study, which focuses on the development of a reliable identification procedure with particular attention to the cancellation effects between different coefficients and to the possible advantages provided by the adoption of CFD simulated manoeuvres (better quality of data, availability of separated forces, etc.). It is believed that the general results obtained are not affected by the discrepancy between CFD simulations and experimental results.

## 2.2. System based modular model

The manoeuvring mathematical model adopted is described in [32] and [33]. The model is based, as usual for manoeuvrability problems, upon the classical equations of motion, considering the 3 degrees of freedom on the horizontal plane (surge, sway and yaw). In particular, considering the Earth-fixed Cartesian frame ( $X_0$ ,  $Y_0$ ,  $Z_0$ ) and the moving reference frame ( $x$ ,  $y$ ,  $z$ ), whose origin is located at  $L_{BP}/2$ , as shown in Fig. 5, the force and moment equations for the ship motions are those shown in Eqs. (1)–(3), where  $X$ ,  $Y$  and  $N$  are hydrodynamic forces and moment respectively; subscripts H, P and R refer to hull, propeller and rudder;  $u$ ,  $v$ ,  $r$  are longitudinal and lateral speed and yaw rate respectively;  $R_T$  is the ship resistance; the terms  $m$  and  $I_Z$  are respectively the mass and the mass moment of inertia (with respect to the vertical axis) of the ship;  $X_{\dot{u}}$ ,  $Y_{\dot{v}}$  and  $N_{\dot{r}}$  are the acceleration derivatives, and  $x_G$  is the longitudinal coordinate of the centre of gravity;  $n$  is propeller revolutions,  $\delta$  is rudder angle.

$$(m - X_{\dot{u}})\dot{u} - m(vr + x_Gr^2) = X_P(u, v, r, n) + R_T(u) + X_R(\delta, u, v, r) + X_H(u, v, r); \quad (1)$$

$$(m - Y_{\dot{v}})\dot{v} + mx_G\dot{r} + mur = Y_P(u, v, r, n) + Y_R(\delta, u, v, r) + Y_H(u, v, r); \quad (2)$$

$$(I_Z - N_{\dot{r}})\dot{r} + mx_G\dot{v} + mx_Gru = N_P(u, v, r, n) + N_R(\delta, u, v, r) + N_H(u, v, r); \quad (3)$$

It has to be remarked that the proposed model is valid for a ship geometrically symmetric with respect to the midship plane, as the one considered in present study. Moreover, the remaining 3 degrees of freedom are not included in this work, considering pitch and heave motions not very important for a displacement ship and neglecting the effect of roll. This assumption is acceptable, at least as long as heeling angles are small, i.e. when speed is not too large and/or the metacentric height ( $GM$ ) is sufficiently high, like in the present case.

The hull hydrodynamic manoeuvring forces are formulated by means of the polynomial approach, described in this case by the following set of equations:

$$X_{HULL} = X_{vv}v^2 + X_{vr}vr + X_{rr}r^2 \quad (4)$$

$$Y_{HULL} = Y_{vv}v + Y_{rr}r + Y_{vv}v|v| + Y_{rr}r|r| + Y_{vrr}vr^2 + Y_{vr}|v|r \quad (5)$$

$$N_{HULL} = N_{vv}v + N_{rr}r + N_{vv}v|v| + N_{rr}r|r| + N_{vrr}vr^2 + N_{vr}|v|r \quad (6)$$

The values of coefficients utilized in present study as initial guess in the SI were evaluated according to Ankudinov et al. [34].

The ship resistance has been directly measured from model tests. Propeller thrust is obtained in terms of RPM and advance velocity by means of the well-known Wageningen series open water diagrams. The evaluation of the propeller lateral forces follows the Ribner theory for propellers in an oblique flow [27].

Rudder forces (drag and lift) are calculated by means of the large amount of experimental data reported in [35]. The flow speed at rudder is computed considering the longitudinal velocities inside and outside the propeller slipstream, opportunely weighted on the basis of rudder coverage, and lateral speed resulting from ship dynamics. Slipstream tube contraction effect and turbulence correction are also included, following the approach proposed in [36]. Furthermore, the effective rudder angle is computed considering the local drift angle, suitably evaluated including flow straightening effects as proposed in [34].

A complete description of the mathematical model used for the rudders and propellers may be found in [37]; this is omitted in

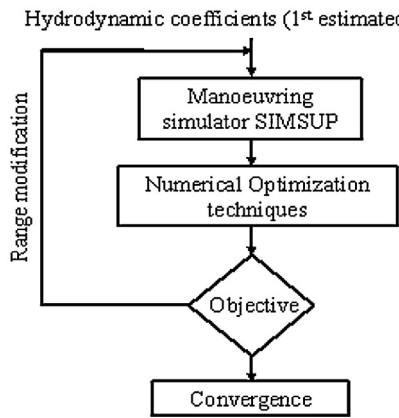


**Fig. 7.** Scheme of the identification procedure with optimization [13].

present work since most of system identifications have been performed imposing rudder and propeller forces, whose mathematical model is therefore not influent.

### 2.3. System Identification by means of genetic algorithm

The SI procedure utilized in the present work consists in the application of the numerical optimization program [38] combined with the system based modular model described in Section 2.2. This procedure was first presented in [11,12], in that case coupled with the simulation program for surface ships SIMSUP [39] developed by CETENA. A successful application to a series of twin screw ships is proposed in [13].

The optimization tool allows to carry out iterative and automatic series of calculations using different programs (in this case the system based simulator) in order to evaluate one or more objective function to be minimized or maximized by means of various optimizations algorithms. In the present work, a Multi Objective Genetic Algorithm has been used. In particular the MOGA-II Algorithm [40,41], available inside ModeFrontier, has been utilized, setting the following internal parameters:

- probability of directional cross-over:	0.5
- probability of selection:	0.05
- probability of mutation	0.1
- DNA string mutation ratio	0.05
- maximum number of generations	50
- size of the initial population	abt. 20

In the present work, different objective functions (see Section 4) representing the discrepancy between the free running manoeuvre obtained by CFD (used as target) and the outcome of the system based model, have been minimized modifying iteratively the values of the hydrodynamic coefficients. In order to clarify the process, in Fig. 6 the scheme used to link the manoeuvring simulation program to the optimization tool is reported.

In particular, the evidenced blocks represent input and output of run in the identification process, while the mean blocks represent intermediate files used; the “HydroCoefficients” block represent the values of the hydrodynamic coefficients, which are initially given in input and automatically modified by the optimization algorithm to reduce the objective functions; “TurningResults” and “ZigzagResults” are the outcomes of the simulation for the turning circle and the zigzag manoeuvre, which vary depending on the hydrodynamic coefficients given in input; finally, “ObjectiveT” and “ObjectiveZ” are the objective functions computed on the basis of the simulation results.

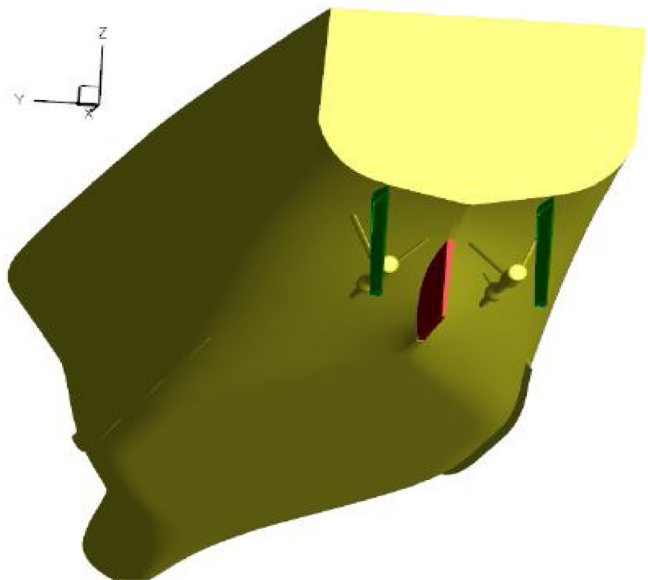


**Fig. 8.** Ship model stern appendages configuration [31].

**Table 3**

Ship model features (geometry and speed conditions).

Ship model features	Symbol	Value
Scale	$\lambda$	25
Length between perpendiculars/beam ratio	$L_{BP}/B$	6.6
Beam/draught ratio	$B/T$	2.89
Block coefficient	$C_B$	0.62
Froude number	$F_N$	0.21
Reynolds number	$Re$	$7.77 \times 10^6$

The identification procedure, schematized in Fig. 7, is structured in general as follows:

- Starting from a relatively large initial range of variation for the investigated coefficients (in this case  $\pm 35\%$  with respect to the value provided by the Ankudinov regression), a large number (200–400) of combinations of hydrodynamic coefficients is generated randomly by the program and corresponding simulations are performed;
- Considering the values of the objective functions in correspondence of the various combinations of hydrodynamic coefficients, the best ones (usually 15) are selected and assumed as input population for the Multi Objective Genetic Algorithm (MOGA);
- The procedure is repeated iteratively with a sequence of MOGA reducing progressively the range of investigation step by step until convergence of each coefficient is reached.

### 3. Test case

A twin screw/twin rudder ship model has been considered in this work (see Fig. 8); the geometrical characteristics of the hull and the speed condition are summarized in Table 3.

Considering this ship model, CFD simulations have been performed in order to provide the input data for the SI procedure, substituting, as already discussed, the experimental tests.

The manoeuvres are simulated at the initial speed  $V_0$  corresponding to a Froude number  $F_N = 0.21$ ; the propeller rate is assumed to be constant during the entire manoeuvring simulation.

In the CFD computations, the physical domain is discretized by means of structured blocks with partial overlap; overlapping grids capabilities are exploited to attain a high quality mesh and for

**Table 4**

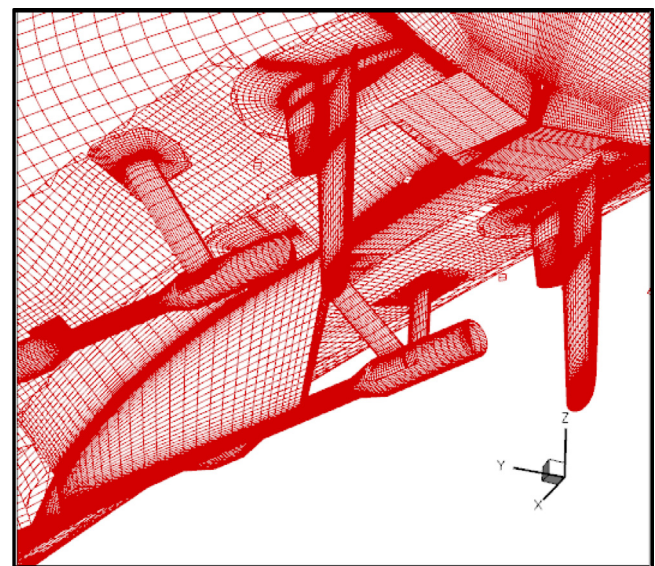
Overlapping blocks: details of the discretization.

Zone	No. of blocks	No. of volumes (Fine)	No. of volumes (Medium)
Background	2	184,320	23,040
Free surface	2	933,888	116,736
Hull	18	2,738,176	342,272
Bilge keels	8	655,360	81,920
Propeller axis	24	733,184	91,648
Actuator disk	2	65,536	8,192
Rudders	208	2,195,456	274,432
Skeg	18	299,008	37,385

refinement purposes. The whole mesh consists of a total of about 7.8 millions of computational volumes. Four grid levels are used for multi-grid acceleration, each being obtained from the finest one by removing every other vertex along each spatial direction. A detail of the discretization of the individual part of the vessel is summarized in **Table 4**. Grid distribution is such that the thickness of the first cell on the wall is always below 1 in terms of wall units ( $y^+ = O(1)$  i.e.  $\Delta/L_{BP} = O(20/Re)$ ,  $\Delta$  being the thickness of the cell). In **Fig. 9** the detailed views of the mesh in the stern region is shown; the use of overlapping grid capability allows taking into account for all the details, in particular for the mesh around the rudder where both the fixed and the mobile parts are carefully discretized.

It is to be pointed out that, instead of generating a fixed background mesh that covers the whole course of the hull, a relatively small background mesh that follows the hull during the motion translating in the horizontal plane and rotating around the vertical axis with the model has been generated. More details about the parameter, the grid and results from these simulations can be found in [29,31,42].

In this work three standard manoeuvres have been considered: the optimization procedure has been applied to two of them at the same time. Namely, the Turning Circle ( $\delta=35^\circ$ ) and the ZigZag 10/10 have been considered since they have opposite characteristics, with high and low rudder angles and consequently high and low sway and yaw speeds. In this way the resulting coefficients in the S.I. have to consider both the large sway and yaw velocities and steady features of Turning, as well as the lower (but more unsteady) values of sway and yaw velocities typical of ZigZag. The estimated manoeuvring coefficients have been verified on a

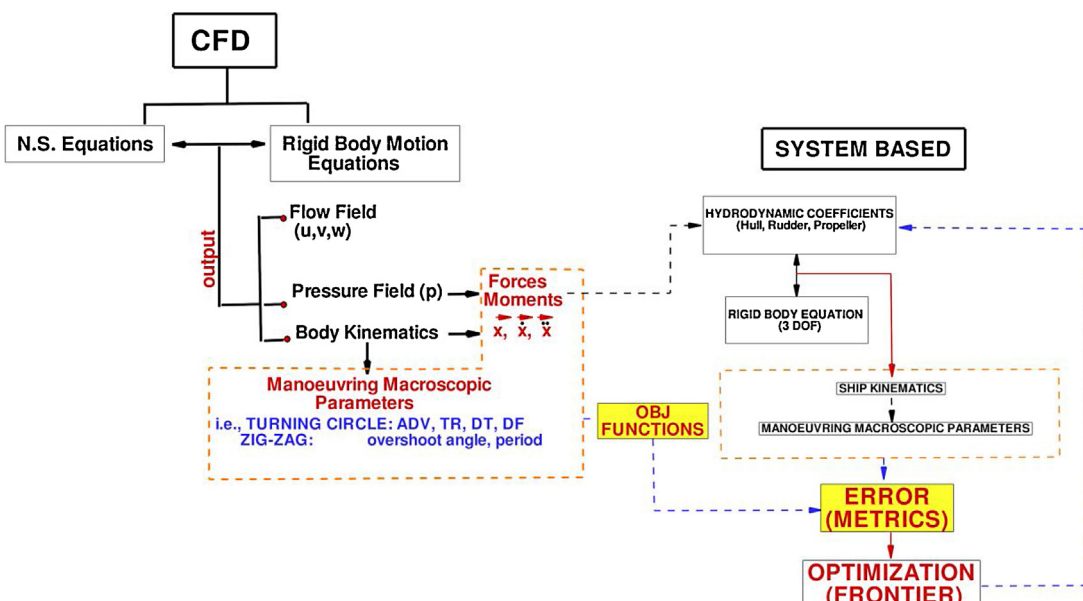
**Fig. 9.** Mesh details in the stern region [31].

third manoeuvre, with features intermediate between these two; namely a ZigZag 20/20. The numerical simulations have been carried out on a parallel machine consisting of 128 processors (16 distributed memory nodes, each node being a 8 cores Intel Xeon CPU X3230@2.66 GHz); computations took about 5 days and six weeks for the medium and finest grid level, respectively.

#### 4. System Identification

System Identification, as described in Section 2.3, has been carried out coupling the modeFRONTIER4 genetic algorithm with the system based model.

Before performing SI, a preliminary sensitivity analysis was carried out ([Appendix A](#)), determining the most important coefficients in the manoeuvrability model considering both ZigZag and Turning Circle manoeuvres. This preliminary step is very useful for the successive identification work, since it allows to understand the behaviour of the adopted model. In fact, the analysis allows

**Fig. 10.** Scheme of the adopted identification procedure, with interactions between CFD and SI.

to take into account, in the optimization procedure, only the most significant hull parameters for the three manoeuvres of interest; in particular, as described in the following, once the most important parameters are chosen, only they are considered in the identification procedure, keeping the remaining constant (equal to the initial guess of the adopted Ankudinov regression) and reducing the occurrence of the cancellation phenomena.

From this analysis it appeared, as obvious, that coefficients related to the rudder force (including flow straightening effects) have a great importance on the manoeuvre. Thus, the first System Identification loops included also rudder related coefficients. However, results were rather poor, with strong cancellation between hull and rudder coefficients. As a result, it was decided to avoid identification of rudder coefficients; this was performed utilizing directly the forces for the rudders and propellers obtained by CFD, exploiting thus the advantage of disposing of separated forces for the various elements. In Fig. 10 the final scheme of the identification procedure is reported, evidencing the interactions with the CFD calculations.

After these preliminary steps, a series of different System Identification loops have been carried out, varying the objective functions considered and the coefficients to be identified.

Initially, only kinematic variables (velocities and trajectory time histories or manoeuvring macroscopic characteristics), have been included into the objective functions algorithms, from which the manoeuvre error is evaluated; then also the hull hydrodynamic forces have been included. The employed objective functions are described in Section 4.1, and are basically different metrics obtained considering the entire time histories of the target and simulated manoeuvre; in addition to this, simpler objective functions, as proposed in [11] based on the main manoeuvring macroscopic data are also considered; the efficiency of the different objective functions was deeply inspected, in terms of their capability in reproducing time histories of the reference CFD manoeuvres. In order to better describe the ship manoeuvring behaviour and then to reduce the discrepancy of simulated and CFD results, hybrid objective functions consisting of a combination of the previous ones were considered.

Finally, in the last identifications series, the hull hydrodynamic forces were considered into the optimization algorithms, in addition to the usual kinematic quantities. The inclusion of these variables was tested in order to perform a gradual constraining to the optimization procedure, with the aim of reducing the cancellation phenomena.

#### 4.1. Identification criteria

The objective functions to be minimized during the optimization procedure have been formulated following two approaches.

In the first one, the error between the target (CFD) and simulated manoeuvre is determined by means of the main macroscopic data of Turning Circle (TC) and ZigZag (ZZ10 and ZZ20 for 10/10 and 20/20 ZigZag manoeuvres) manoeuvres. In Eqs. (7) and (8) the formulations of  $OBJ_{TC}$  and  $OBJ_{ZZ}$  functions for the turning circle and zigzag manoeuvre respectively are reported. They consist in the arithmetic mean of the relative errors of each parameter considered; the signed terms in the equations represent the target parameters

$$OBJ_{TC} = \frac{1}{8} \left( \left| \frac{AV - \bar{AV}}{\bar{AV}} \right| + \left| \frac{TR - \bar{TR}}{\bar{TR}} \right| + \left| \frac{D_T - \bar{D}_T}{\bar{D}_T} \right| + \left| \frac{T_{90} - \bar{T}_{90}}{\bar{T}_{90}} \right| + \left| \frac{T_{180} - \bar{T}_{180}}{\bar{T}_{180}} \right| + \left| \frac{D_F - \bar{D}_F}{\bar{D}_F} \right| + \left| \frac{r_{STAB} - \bar{r}_{STAB}}{\bar{r}_{STAB}} \right| + \left| \frac{V_{STAB} - \bar{V}_{STAB}}{\bar{V}_{STAB}} \right| \right) \quad (7)$$

where  $AV$  is Advance,  $TR$  is Transfer,  $D_T$  is Tactical Diameter,  $D_F$  is Steady Turning Diameter,  $T_{90}$  and  $T_{180}$  are time to reach a  $90^\circ$  and  $180^\circ$  heading change,  $r_{STAB}$  and  $V_{STAB}$  are yaw rate and ship speed in the steady turn.

$$OBJ_{ZZ} = \frac{1}{5} \left( \left| \frac{\psi_{OV1} - \bar{\psi}_{OV1}}{\bar{\psi}_{OV1}} \right| + \left| \frac{\psi_{OV2} - \bar{\psi}_{OV2}}{\bar{\psi}_{OV2}} \right| + \left| \frac{t_{OV1} - \bar{t}_{OV1}}{\bar{t}_{OV1}} \right| + \left| \frac{t_{OV2} - \bar{t}_{OV2}}{\bar{t}_{OV2}} \right| + \left| \frac{T - \bar{T}}{\bar{T}} \right| \right) \quad (8)$$

where  $T$  is period,  $\psi_{OV}$  and  $t_{OV}$  are overshoot angles and times. In the second approach, the metrics objectives are used; in this case, the error represents the distance between target and simulated time histories of the manoeuvring variables comparing the values of the two vectors. Three different metrics have been used [43]: the Euclidean metric ( $L_2$ ) that evaluates the integral over time of the square distance vector (see Eq. (9)); the L-infinity metric ( $L_{\infty}$ ) that considers the largest absolute distance (see Eq. (10)); the Hausdorff distance ( $H$ ) that represents the greatest of all the distances from a point in one vector to the closest point in the other one (Eq. (11)). The Hausdorff metric represents a novelty in SI application to the manoeuvrability problem; in [43] its efficiency was recognized; in particular, the Authors demonstrated that only the Hausdorff metric proved to be sufficiently robust to provide reasonably good results from disturbed time vectors.

$$\rho_{L_2}(x(t), \bar{x}(t)) = \left\{ \int_0^{T_0} [x(t) - \bar{x}(t)]^2 dt \right\}^{1/2}; \quad (9)$$

$$\rho_{L_\infty}(x(t), \bar{x}(t)) = \max_{t \in (0, T_0)} |x(t) - \bar{x}(t)|; \quad (10)$$

$$\rho_H(x(t), \bar{x}(t)) = \max \left\{ \sup_{t_1 \in (0, T_0)} \inf_{t_2 \in (0, T_0)} \rho_0(x(t_1), \bar{x}(t_2)), \sup_{t_2 \in (0, T_0)} \inf_{t_1 \in (0, T_0)} \rho_0(x(t_1), \bar{x}(t_2)) \right\} \quad (11)$$

where  $\rho_0$  is a metric typically defined as  $\rho_0 = |x(t) - \bar{x}(t)|$ , and  $x$  is a chosen variable of interest (e.g. a coordinate, a velocity, etc.).

In the present work, the variables involved in the metrics formulations are the kinematic ones, the velocity components  $u(t)$ ,  $v(t)$ ,  $r(t)$  and the positions  $X_0(t)$ ,  $Y_0(t)$  in the form of absolute space distance vector  $d(t)$  in the horizontal plane. It has to be remarked that in [43] the trajectory variables were not considered, since they are sensitive to the initial conditions of the velocity components. In the present work, this was not considered an issue, being the numerical data used as input for the identification not affected by noise. In one of the identification loops (see Section 4.2), also the dynamic quantities, i.e. the hull hydrodynamic force and moment components  $Y_{HULL}(t)$  and  $N_{HULL}(t)$  have been taken into account in the metric algorithms.

As a general remark, the possibility to include the components of the speed vector (instead of the resultant) within metric algorithms allows to better consider the hydrodynamic phenomena of the manoeuvre: in fact, the knowledge of  $u(t)$  and  $v(t)$ , together with the yaw rate  $r(t)$  allows to determine more accurately the sway-yaw response of the ship as well as to define uniquely and with great accuracy the drift angle of the vessel. The drift angle may be also available when experimental data are considered, however it is usually obtained processing data and not as a direct measurement, thus being intrinsically more noisy and more subject to errors. This detail may significantly improve the characterization of all the quantities involved in the ship manoeuvrability.

**Table 5**

List of system identifications carried out from CFD free-running model tests.

ID		Model	Objective functions configuration	Coefficients
1	A	Model 0	OBJ <sub>TC</sub> ; OBJ <sub>ZZ10</sub>	$N_r N_v Y_r Y_v N_{rv} Y_{vv} Y_v$
	B			$N_r N_v Y_r Y_v N_{rv} Y_{vv}$
2	A	Model 1	Euclidean $L_2(u, v, r, X_o, Y_o)$	$N_r N_v Y_r Y_v N_{rv} Y_{vv}$
	B		L-infinity $L_{\infty}(u, v, r, X_o, Y_o)$	
	C		Hausdorff $H(u, v, r, X_o, Y_o)$	
	D		OBJ <sub>TC</sub> – OBJ <sub>ZZ10</sub>	
3		Model 1	$L_2(u, v, r); H(X_o, Y_o)$	$N_r N_v Y_r Y_v N_{rv} Y_{vv}$
4		Model 1	$L_2(u, v, r, Y_H, N_H); H(X_o, Y_o)$	$N_r N_v Y_r Y_v N_{rv} Y_{vv}$

#### 4.2. System Identification procedures

Four different identification series have been carried out; they differ for the identified coefficients set, the objective functions considered and the manoeuvring model utilized to perform the simulations; the various combinations of them are listed in Table 5.

For what regard the manoeuvring model, as anticipated, the study may be subdivided into two successive phases, which consider two different manoeuvring simulation models: the first part (consisting of ID1.A and ID1.B) was carried out utilizing the original system based modular mathematical model (see Section 2.2), herein called *Model 0*. In the second part (consisting of ID\_2, ID\_3 and ID\_4) the original manoeuvring model was modified substituting propellers and rudders forces by those computed directly by CFD, resulting in a sort of hybrid model, with hull forces according to the original mathematical model and rudder/propeller forces according to CFD. Moreover, in order to eliminate, as much as possible, discrepancies between model behaviour and CFD manoeuvres, in this second phase the longitudinal hull manoeuvring forces were pre-calibrated before running the actual identification procedures. The new manoeuvring model has been denoted as *Model 1*.

The values of the metrics considered during the identifications are relative values; in particular, they have been nondimensionalised with respect to the initial value obtained using the initial coefficients set from Ankudinov regression. This has been done in order to obtain comparable values for all the metrics, which is important when considering averages in order to attribute the same weight to all terms. In fact, in ID2 and ID3 a unique metric objective function has been measured for the speed components  $u(t)$ ,  $v(t)$ ,  $r(t)$ , averaging the metric values; the trajectory objective has been considered separately. The same approach has been utilized in ID4 for the hull loads  $Y_{HULL}(t)$  and  $N_{HULL}(t)$ , but in this case the trajectory metric has been averaged with the velocities ones, in order to have at most four objective functions (two for each manoeuvre) into the optimization procedure.

##### 4.2.1. Preliminary results (Model 0)

In the first identification loops ID\_1A and ID\_1B the original mathematical model (*Model 0*) has been considered; since this first series of identifications presented some problems, the complete results are omitted for the sake of shortness, while a discussion of the main outcomes is reported in the present section.

In both cases (ID\_1A and ID\_1B), 6 hydrodynamic coefficients were considered, i.e. the 4 linear coefficients plus two second order coefficients, chosen on the basis of the sensitivity analysis. In addition to this, in ID\_1A the straightening coefficient  $\gamma_v$  was considered; this was chosen as most important coefficient for rudder forces, considering that the open water rudder is represented in a sufficiently accurate manner on the basis of previous results.

Considering the results of the two identification loops, the inclusion of a rudder related coefficient led to worse results with respect to ID\_1B, as reported in Table 6. In the table the errors (in terms of macroscopic parameters) for the two identified manoeuvres and for

the third one used for verification are reported: they show clearly that a certain improvement is obtained with respect to the original error with the direct application of hydrodynamic coefficients from Ankudinov regression (indicated as Regression in the table). However, a rather high mean error is still present, which is even higher in the ID1.A case; this confirmed that the simultaneous identification of hull and rudder parameters is rather difficult, being affected by greater cancellation phenomena between coefficients.

Both procedures showed a large residual error from CFD simulations after identification, especially in the more unsteady ZigZag manoeuvres; this is a consequence of the different description of the rudder forces between CFD and system based modular mathematical model. In order to deeply analyze the differences existing between the models behavior, rudders forces during Turning were evaluated at the same kinematic conditions of the CFD simulation (i.e. imposing the velocities obtained in the CFD calculations). The sum of the starboard and port rudders forces (both the longitudinal component and the lateral one) estimated through the simplified model, are quite different from the CFD time histories (see Fig. 11). This may be probably due to the fact that the system based modular model considers mean velocity components on the rudders that, although corrected with the propeller action and the hull straightening effect, do not describe the complex phenomena of the flow field in the stern region. As a result, the rudders result more efficient in the system based mathematical model with respect to the CFD data, with higher lift and drag forces values during both the stabilized phase (with higher mean value) of Turning and the transient phase (with higher peaks). Moreover, it is clear that the system based modular mathematical model does not keep into account the asymmetry of rudder loads between starboard and port side. This asymmetry is typical in twin screw ships, in which a considerable difference of the flow direction during turn at the two rudder locations is present. In this case the external rudder loads greatly decrease because the flow incidence angle is lower with respect to the internal one, that is influenced by the hull straightening effect.

It is obvious that, from the point of view of the System Identification, the above mentioned differences can significantly affect the whole procedure, the estimated value of the hull hydrodynamic coefficients being altered by the over prediction of the rudder forces. This analysis led to the decision to replace rudders and propellers forces in the system based modular model with the CFD estimations, and to keep only the hull model for the identification. In this way the hull coefficients are identified avoiding the possibility of compensation effects with control devices, allowing to better analyze the merits of the various objective functions adopted.

Before performing the identification procedures of the second phase, a further calibration of the model was carried out, considering the longitudinal added resistance caused by sway-yaw motions. In order to do this, the values of the hydrodynamic coefficients  $X_{vv}$ ,  $X_{vr}$  and  $X_{rr}$  for the evaluation of the longitudinal hull force were opportunely tuned. In particular, the sole longitudinal equation of

**Table 6**

ID1 manoeuvring errors based on the macroscopic characteristics of TC, ZZ10, ZZ20.

Coefficients set	OBJ_TC	OBJ_ZZ10	OBJ_ZZ20	Average
Regression	0.093	0.547	0.537	0.392
ID1_A	0.061	0.198	0.385	0.215
ID1_B	0.033	0.107	0.371	0.171

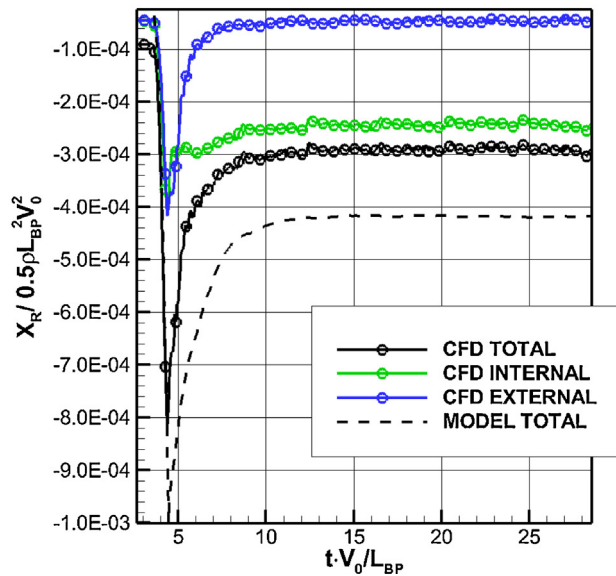
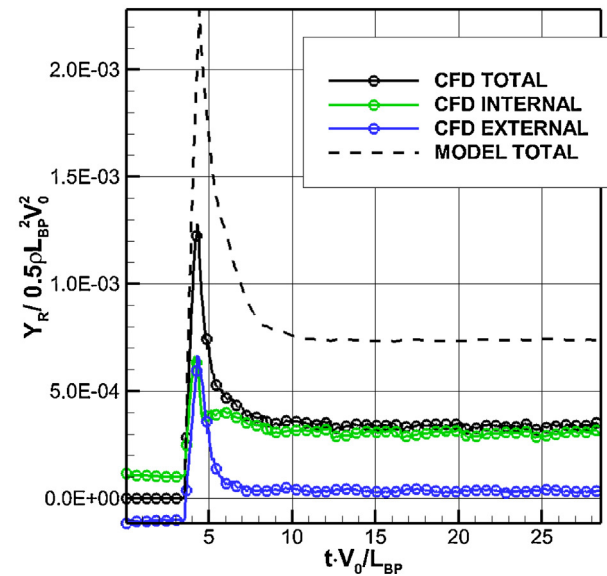
**a****b**

Fig. 11. Time histories of Turning Circle ( $\delta=35^\circ$ ) rudders longitudinal (a) and lateral (b) forces; system based modular model vectors have been evaluated imposing the same kinematic conditions of the CFD simulations.

motion (1) was considered, imposing  $v(t)$  and  $r(t)$  time histories obtained from CFD Turning simulation and evaluating numerically the longitudinal speed variation in time; all the coefficients were modified by a common factor  $\lambda_X$ . The longitudinal hull force is then evaluated as reported in (12); the value of the coefficient  $\lambda_X$  was obtained imposing the same speed drop obtained in the CFD calculations.

$$X_{HULL} = \lambda_X (X_{vv} v_{CFD}^2 + X_{vr} v_{CFD} r_{CFD} + X_{rr} r_{CFD}^2) \quad (12)$$

The result of this activity is summarized in Fig. 12: the simulation results before and after the calibration of the longitudinal coefficients are shown, compared to the target CFD time history.

This calibration is important in view of the identification activity, because the different surge speed could have affected the estimation of lateral force and yaw moment hydrodynamic coefficients. Thanks to this preliminary tuning based on CFD simulations, the identification of longitudinal force hydrodynamic coefficients can be avoided, thus limiting the amount of coefficients to be considered.

#### 4.2.2. Identification results with Model 1

After the two model modifications described in Section 4.2.1, the other identification loops (ID\_2 ID\_3 and ID\_4) have been performed. In particular, in ID\_2 group, the results obtained adopting the four different objective functions (three metrics and the macroscopic parameters based objectives) are reported. In ID\_3 an example of hybrid objective function with the use of two different metrics for different variables is reported; finally, in ID\_4 the results in case of inclusion of hull forces in the metrics are reported. In the present section, the main outcomes are summarized, while the complete results are reported in Appendices B and C respectively for ID2 and ID3/ID4 results.

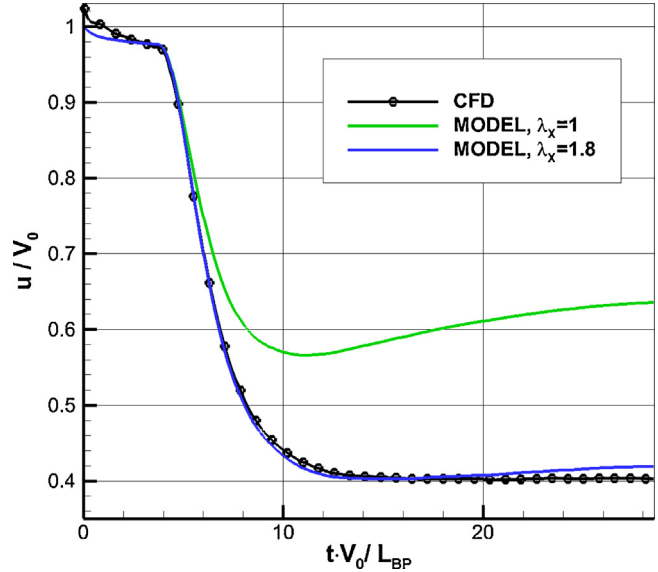
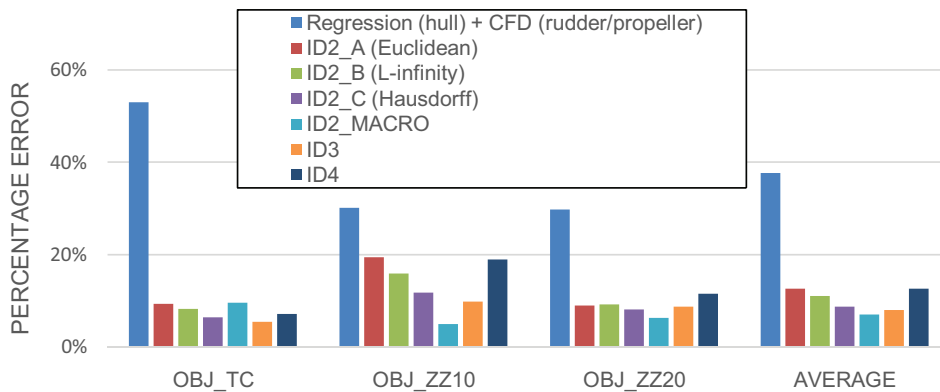


Fig. 12. Comparison at same kinematic of Turning speed drops.

As a general remark, the utilization of *Model 1* provided very different results when compared to the first ID1 identification loops, both in terms of manoeuvre errors and hull coefficients variation.

In Table 7 the variations of coefficients value with respect to the initial guess (Ankudinov regression) obtained in all the identification loops is reported. In Table 8 the residual differences of the Turning Circle and ZigZag manoeuvres are reported for ID\_2, ID\_3 and ID\_4, and for the hybrid model with hull forces evaluated on the basis of Ankudinov regression and rudder/propeller forces from



**Fig. 13.** Histogram of the manoeuvring errors based on the macroscopic characteristics.

CFD (indicated as “Regression (hull) + CFD (rudder/propeller)”). The same data are reported in Fig. 13 for better clarity.

It is clear that the coefficients variation trends for the yaw related coefficients  $N_r$ ,  $N_{rv}$ ,  $N_v$ , considering the results obtained with the modified simulator *Model 1*, are opposite to those obtained with *Model 0*. Moreover, the manoeuvres errors are greatly reduced with respect to ID1, confirming that a not correctly captured rudders/propellers behaviour can lead to a misleading identification of the hull dynamic response, or even to prevent it. The different values of the hydrodynamic coefficients in ID.1 group and in the remaining ones are due to a compensation of the error in the rudder loads, which is clear considering the yaw moment coefficients. In particular, in ID.1 the resistance to yaw is increased to compensate the higher rudder force in the simulator. However, this does not allow obtaining satisfactory reductions of errors for all manoeuvres, with ZigZag manoeuvres presenting residual errors ranging from 20% to 40%. On the contrary, with the other identification loops the yaw related coefficients vary less and the errors of all manoeuvres are brought to values lower than 10% in most cases.

Considering differences between *Model 1* and *Model 0*, it has to be underlined that the initial error with the modified model (Regression (hull) + CFD (rudder/propeller) in Table 8) is of the same order of magnitude of the previous one with *Model 0*, even if with different (and more uniform) errors for the various manoeuvres. This underlines that the differences between simulated and CFD manoeuvres are due not only to the control devices forces, but also to the hull response.

Considering the ID.2 group, as it can be noticed looking at the manoeuvring plots in Appendix B, the use of  $OBJ_{TC}$  and  $OBJ_{ZZ10}$  (macroscopic parameters objective) allows to reproduce the trajectories with a better agreement (Fig. 21), whereas it does not provide equally satisfactory results in terms of velocity components (Fig. 22a–c, Fig. 23a–c and Fig. 24a–c), with larger discrepancies than the ones obtained with the metrics. On the contrary, metric objectives are particularly efficient in capturing the time histories of the speed components but less capable to reproduce the reference trajectory. Among all the metrics, Hausdorff distance seems to be better than the others in reproducing the trajectories, especially for the Turning Circle manoeuvre; on the contrary Euclidean or L-infinity metrics are not able to correctly minimize the error in the Turning trajectory; this is due to the fact that these two metrics are concurrent with respect to  $OBJ_{TC}$ , thus their minimization leads to higher value of  $OBJ_{TC}$  itself.

This is clarified in Figs. 14 and 15, where the outcomes of the optimization procedure are represented. In particular, each point represents a set of hydrodynamic coefficients tested in the optimization loop; in Fig. 14, the values of  $OBJ_{TC}$  and the Euclidean metric are represented, while in Fig. 15 values of  $OBJ_{TC}$  and the Hausdorff metric are represented. As it can be seen, this

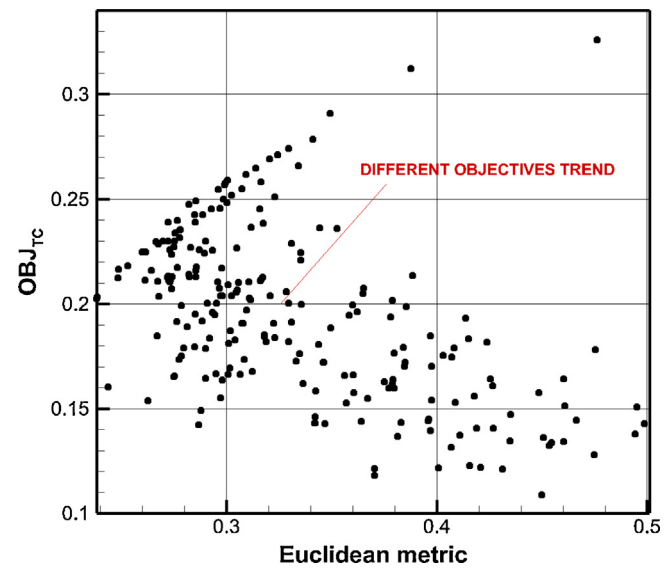


**Fig. 14.** ID2 designs scatter diagrams of  $OBJ_{TC}$  objective function with respect to Euclidean metric.

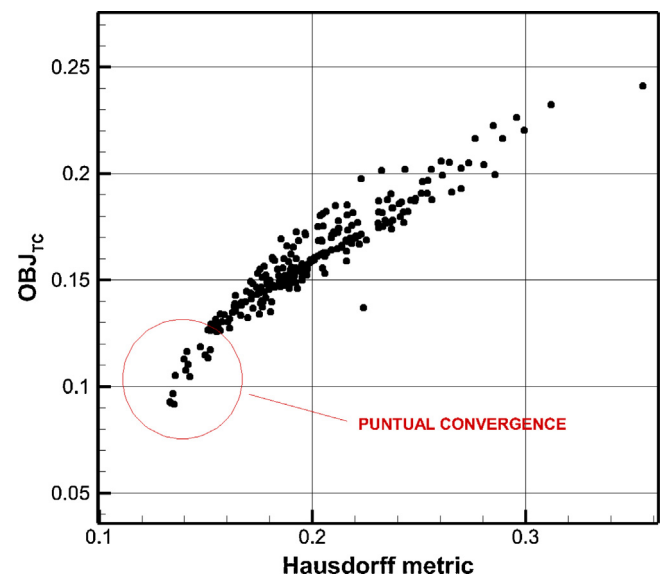


**Fig. 15.** ID2 designs scatter diagrams of  $OBJ_{TC}$  objective function with respect to Hausdorff metric.

**Table 7**

Manoeuvring coefficients percentage relative variation with respect to regression value.

Coefficients set	$N_r$	$N_{rv}$	$N_v$	$Y_r$	$Y_{rv}$	$Y_{vv}$	$\gamma_v$
ID1_A	54.0%	23.0%	108.0%	-6.0%	-72.0%	-42.0%	4%
ID1_B	41.2%	44.8%	49.5%	-59.9%	-74.0%	-77.6%	-
ID2_A (Euclidean)	-36.1%	-52.2%	-32.9%	-30.6%	-46.8%	-51.3%	-
ID2_B (L-infinity)	-45.0%	-52.5%	-45.5%	1.9%	-56.0%	-55.4%	-
ID2_C (Hausdorff)	-37.1%	-57.3%	-33.3%	-54.6%	-13.7%	-88.5%	-
ID2_D (macro)	-34.6%	-76.1%	-22.2%	-77.9%	-3.8%	-20.3%	-
ID3 (Euclidean/velocities + Hausdorff/trajectory)	-57.5%	-54.7%	-46.4%	-32.1%	-38.6%	-53.7%	-
ID4 (Euclidean/velocities/forces + Hausdorff/trajectory)	-47.5%	-60.3%	-47.7%	-48.0%	-54.8%	-52.7%	-

**Table 8**

Manoeuvring errors based on the macroscopic characteristics for TC, ZZ10, ZZ20 and averaged values.

Model	Coefficients set	OBJ_TC	OBJ_ZZ10	OBJ_ZZ20	AVERAGE
0	Regression	0.093	0.547	0.537	0.392
	ID1_A	0.061	0.198	0.385	0.215
	ID1_B	0.033	0.107	0.371	0.171
1	Regression (hull) + CFD (rudder/propeller)	0.531	0.302	0.298	0.377
	ID2_A (Euclidean)	0.094	0.195	0.090	0.126
	ID2_B (L-infinity)	0.083	0.160	0.092	0.111
	ID2_C (Hausdorff)	0.064	0.118	0.081	0.088
	ID2_D (macro)	0.096	0.050	0.063	0.070
	ID3 (Euclidean/velocities + Hausdorff/trajectory)	0.055	0.098	0.088	0.080
	ID4 (Euclidean/velocities/forces + Hausdorff/trajectory)	0.072	0.190	0.116	0.126

representation clearly evidences the concurrence of the two objectives (in particular,  $L_2$  values decrease and  $OBJ_{TC}$  values increase and vice versa); the various points dispose on a sort of Pareto front. On the contrary, Hausdorff metric presents a different trend, having the same tendency of the  $OBJ_{TC}$  value, with the coefficients sets converging toward a unique point; this means that a minimization of the Hausdorff metric leads also to a minimization of the value of  $OBJ_{TC}$ .

These different behaviours can be explained looking at Fig. 16: Euclidean metric evaluates an errors vector by comparing elements at the same time instants; Hausdorff metric generates an error vector consisting of the smallest distances between the two time histories considered, neglecting the correspondence of time instants. For this reason, the Euclidean metric is not effective when applied to position vectors because it compares elements that often belong to different parts of the trajectory, especially in those cases where the simulated and the reference manoeuvres differ from each other for the surge speed. Turning Circle manoeuvres that are in better accordance to the reference ones in terms of Tactical Diameter, advance and transfer, could present high values of the metric in case a different speed is present and vice versa (i.e. it could have high  $OBJ_{TC}$  but low metric values when the elements are similarly disposed in time).

This ambiguity is eliminated utilizing the Hausdorff metric. The Hausdorff metric minimizes a manoeuvre error that is always evaluated between the homologous points of the paths, even if the ship speed is different: in this way, the macroscopic characteristics of the trajectory are correctly described, and both  $OBJ_{TC}$  and the Hausdorff metric values are minimized. It has to be underlined that this may not mean that the Hausdorff metric is better, since a correct representation of the trajectory with a wrong representation of the velocity has to be considered as a not satisfactory result.

In the ZigZag manoeuvres this problem is less marked, also because the differences of the ship surge speed are usually lower with respect to tight manoeuvres as Turning.

On the basis of these considerations, hybrid objective functions configurations were adopted, with the aim to improve the reproduction of the various manoeuvring quantities. In ID3, in particular, Hausdorff metric was used for the positions time histories  $X(t)$  and  $Y(t)$ , and Euclidean metric for speed components  $u(t)$ ,  $v(t)$  and  $r(t)$ .

The Euclidean metric was preferred to  $L_{INF}$  because it evaluates a global distance considering the entire simulation time. Furthermore,  $L_{INF}$  metric shows a minor robustness in the coefficients evaluation with respect to the other identifications: the resultant coefficients by using the metric  $L_{INF}$  are rather different with respect to other cases (see Table 7), with higher variations which may evidence a higher cancellation effect.

As it is possible to see from manoeuvring plots of Appendix C (Figs. 25–28) and from Table 8, for both Turning Circle and ZigZag obtained with the hydrodynamic coefficients resulting from the identification with the hybrid objectives, the errors on the manoeuvre decrease with respect to the single metric cases. In general, a better correspondence of trajectories is achieved (being only worse than the objective function with macroscopic parameters for the zigzag manoeuvres), maintaining the correct evaluation of ship speeds already remarked before. As a consequence, the proposed strategy with the hybrid metrics seems to provide the best results among the ones analyzed, allowing to exploit the merits of the two metrics and to reduce the possible shortcomings.

Considering the problem of cancellation between different coefficients, it has to be remarked that, analysing the two groups of identification (ID2 and ID3) a similar coefficients variation trend is recognizable. This may indicate a certain robustness of the optimization algorithm and then the validity of the identification procedure previously described. Although this may be considered a satisfactory result, it has to be pointed out that the coefficients evaluation is probably still affected by some cancellation phenomena, especially between the most important hull parameters, i.e.  $N_r$  and  $N_v$ . This is confirmed by  $N$  hull force curves (see Fig. 22f, Fig. 23f, and Fig. 24f), that are almost coincident, despite the different values of coefficients, because of the cancellation effects among  $N$  coefficients that vary maintaining the same ratio. In general, the variation of the  $Y$  coefficients is more marked, showing again cancellation effects, together with the minor importance of these coefficients in the manoeuvre dynamic; a clear example of this is shown in Fig. 17, in which the successive steps of identification from the initial set to the last MOGA are shown in terms of range of values of the coefficients considering the best 15 sets in each optimization step. It is clear from the figure that the two  $N$  coefficients have a similar trend (maybe due to cancellation), but

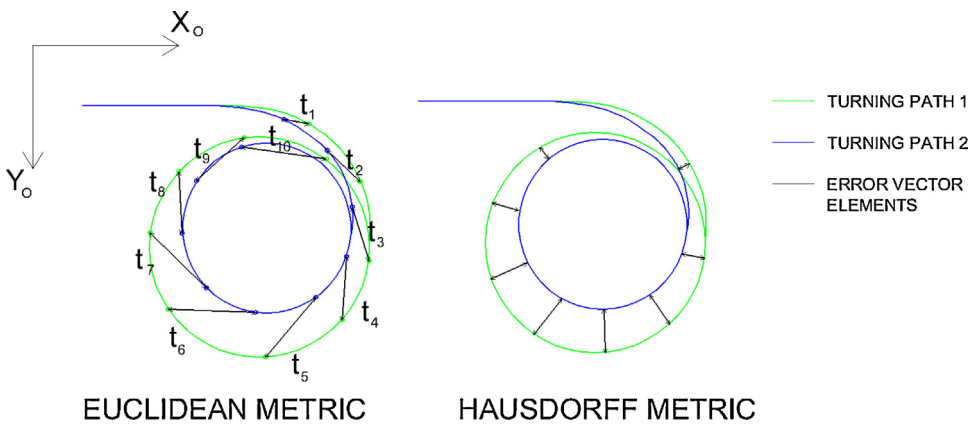


**Fig. 16.** Euclidean and Hausdorff algorithms applied to two generic turning paths.

reaching at each time a good convergence; on the contrary, the  $Y$  coefficients (and  $Y_r$  in particular) do not converge completely at the end of each step. For these coefficients, it appears that the actual possibility of identification is a larger problem than cancellation phenomena.

Considering the above mentioned problems, results obtained in ID2 and ID3 steps were already rather satisfactory, but still needing some improvement, especially regarding possible cancellation effects; in order to find an additional way to constrain the problem and limit them, a further step was considered. In the last ID4 identifications, in addition to the kinematic parameters, hull hydrodynamic forces  $Y_{HULL}(t)$  and  $N_{HULL}(t)$  from CFD were also considered into the objective functions (see Table 5). Unfortunately, this procedure did not lead to an improvement in manoeuvres simulation (Figs. 25–28), presenting slightly higher errors with respect to ID3, where only kinematic quantities were considered. Although the procedure has been constrained considering the  $Y_{HULL}(t)$  and  $N_{HULL}(t)$  metrics, the hull loads did not get closer to the CFD

target, contrarily to what expected. This apparently anomalous result is due to the fact that the objectives depending on hull loads for Turning Circle and ZigZag manoeuvres are concurrent during the optimization procedure (i.e. minimizing the error for forces of Turning Circle leads to higher errors in ZigZag forces, and vice versa). This leads, at the end, to a slightly lower accuracy in the manoeuvres definition, increasing the objectives average values (see Table 8). This unfavourable behaviour is confirmed by a deeper analysis carried out performing identification considering only the hull forces. In this case, hydrodynamic coefficients are modified during SI in order to reduce the discrepancy between the time histories of hull forces from CFD (reference, as before) and from the system based model, imposing the same kinematics of CFD simulations, as already done for  $X$  coefficients calibration and for rudder models comparison. The various sets of hydrodynamic coefficients obtained in this analysis dispose on the Pareto frontier in TC-ZZ10 objectives space, as reported in Figs. 18 and 19, in which the values of the different metrics for the different sets of coefficients is reported. This

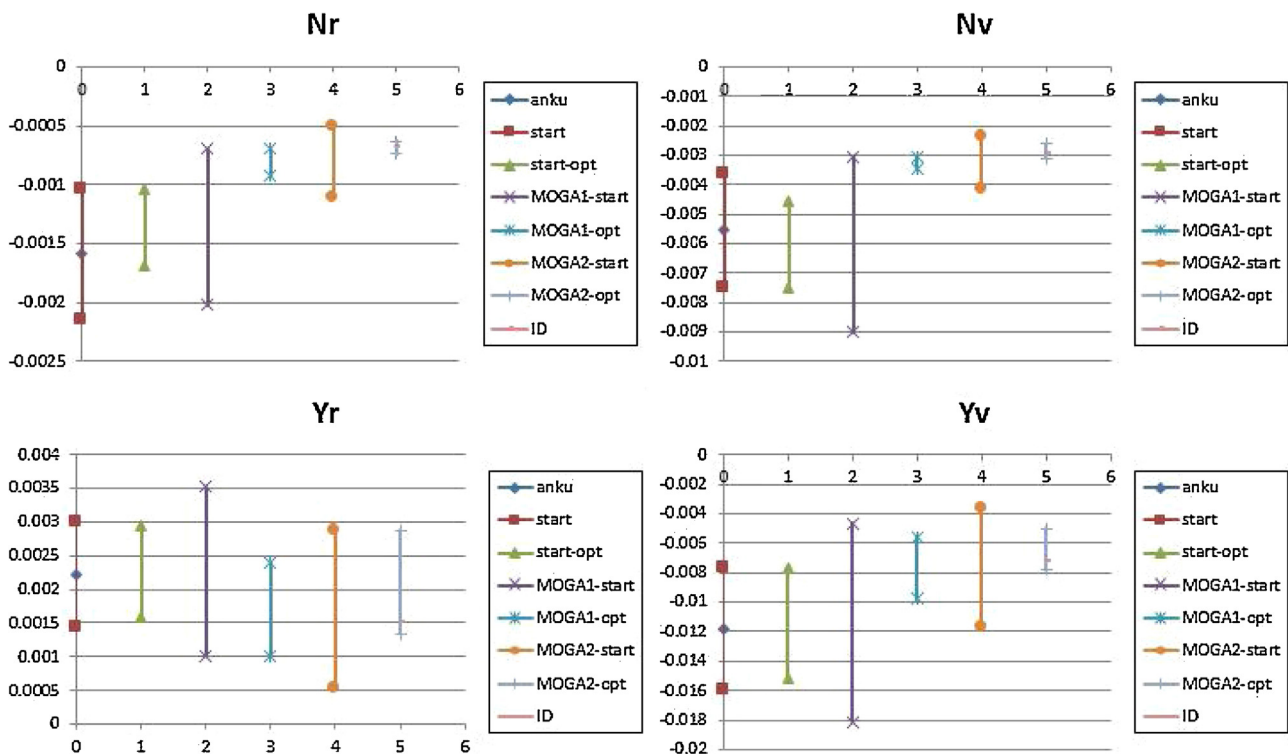


**Fig. 17.** Variation of linear coefficients during the optimization phases of ID3.

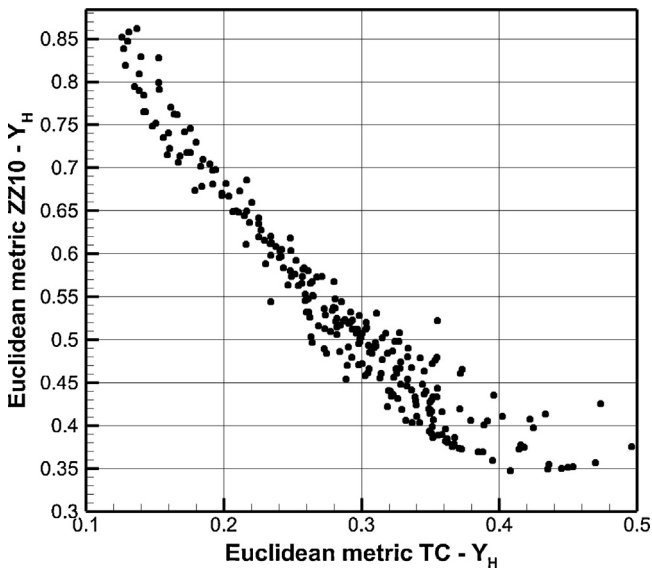


**Fig. 18.** Design scatter diagrams for TC ( $\delta = 35^\circ$ ) and ZZ10 metric objectives of sway lateral force.

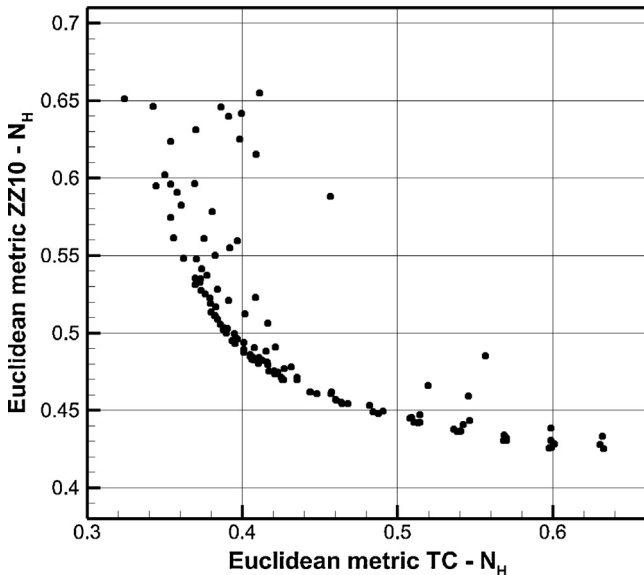


**Fig. 19.** Design scatter diagrams for TC ( $\delta = 35^\circ$ ) and ZZ10 metric objectives of yaw moment.

means that the ship under analysis shows very different characteristics between manoeuvres with high and low deviations from the rectilinear motion (i.e. higher and lower values of yaw and sway velocities), and the polynomial parameters considered in the identification loop for hull loads are not able to capture at the same time these two different manoeuvring behaviours. Correspondingly to a worse replacement of the reference manoeuvres, there are no remarkable improvements in the evaluation of the hydrodynamic coefficients, being still affected by cancellation phenomena.

## 5. Conclusions

In this work the use of data provided by U-RANSE simulations of free running manoeuvres for the identification of the manoeuvring hydrodynamic coefficients was investigated. In particular, the results of the CFD simulations were included as reference values in

objective functions formulated both in terms of weighted averages of macroscopic manoeuvring parameters and vectors consisting of the instantaneous values of kinematic vectors describing the response of the vessel.

The use of CFD simulated manoeuvres as quasi-trials resulting in kinematic responses input for System Identification appears very helpful; in fact it is possible to obtain a huge amount of data (less noisy than experimental ones) by which the optimization procedure can be constrained. This may be useful both for the optimization algorithm itself and to improve the accuracy of manoeuvring simulations of the simplified models, allowing to stress their possible limits, as evidenced in the case of the rudder force discussed.

Nevertheless, CFD tools still show the need for an improvement, especially when dealing with manoeuvres with large unsteady parts such as the ZigZag manoeuvre; in particular, a better simulation of the propeller might allow to improve simulation results; this activity will be carried out in future work. It is believed in general that, considering the trend in the last decade, with always improving CFD tools and with the availability of more powerful computational resources, CFD will represent in future a very useful tool also for the designer, not only limited to the research side.

This study shows that System Identification is particularly efficient for the prediction of the manoeuvring characteristics when applied to the single ship, confirming the validity of previous works [16]. However, the identifications were also focused on the hull coefficients estimation: in order to conceive a method for off-line System Identification with a high robustness, even if in some cases at the expense of the accuracy in the manoeuvres simulation, the number of parameters for the optimization designs has been reduced as much as possible, and the mathematical model and the identification procedure has been gradually constrained, with the purpose to reduce cancellation phenomena.

The results obtained with the various procedure point out that the problems related to cancellation phenomena are still to be completely solved. However, the results obtained with the majority of methods developed show similar trends of variation of the coefficients, allowing to conclude that the procedure outlined is promising. In particular, the hybrid metric approach, with a combination of Hausdorff metric and Euclidean metric for trajectory and velocity variables appeared the best solution, allowing to exploit the advantages of both metrics.

The inclusion of hull forces in the identification algorithm did not allow to reduce cancellation phenomena, but on the contrary evidenced rather large differences in optimal coefficients among manoeuvres with high and low values of sway and yaw velocities; this suggests the need for the introduction of different models (with respect to the one adopted) for the forces representation. This issue will be object of future activities.

## Appendix A. Sensitivity analysis

As reported in the main text, a sensitivity analysis was carried out in a preliminary phase; this allowed to evaluate the most significant manoeuvring hydrodynamic coefficients for the ship considered and for the mathematical model adopted. The sensitivity analysis was carried out evaluating the variation of the manoeuvrability macroscopic data in correspondence to a perturbation of the value of each coefficient of the original regression. In this analysis all manoeuvring coefficients were considered; moreover, in order to consider the importance of rudder action and hull straightening effect on the manoeuvring response, the lift derivative  $\partial C_L / \partial \alpha$  and the two hull straightening coefficients  $\gamma_v$  and  $\gamma_r$  were also taken into account. Each coefficient was varied separately (keeping the remaining constant) by 10% with respect to

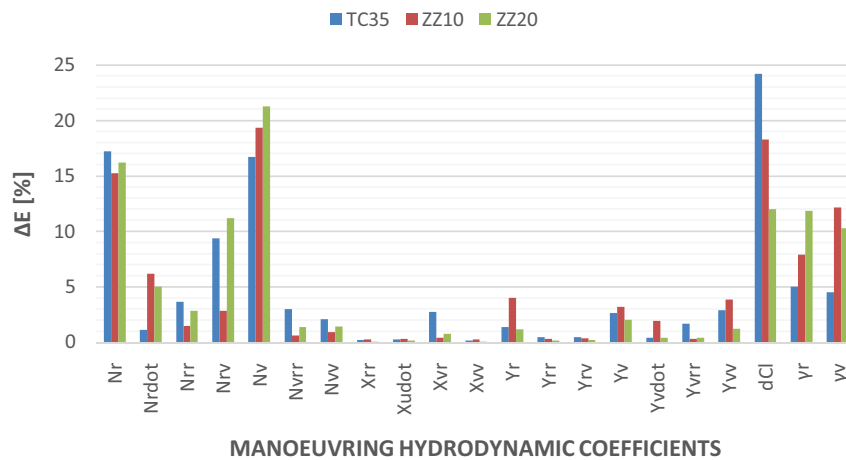


Fig. 20. Histogram of the sensitivity analysis results.

the original value, obtaining as many simulations as the number of parameters considered. This is a fundamental step before proceeding with the study of System Identification methodologies, because it allows to gain a deeper insight on the kinematic nature of the three manoeuvres.

The manoeuvring data modification for each coefficient variation was quantified through Eq. (13);  $E$  is the manoeuvre variation in absolute value, and  $\Delta E$  represents the relative deviation with respect to the total sum of the variations obtained for the different coefficients, allowing to rank easily the importance of the various coefficients;  $i$  denotes the  $i^{\text{th}}$  coefficients analyzed.

$$\Delta E_i = \frac{E_i}{\sum_i E_i} \quad (13)$$

In this way it is possible to easily compare on the single manoeuvre the influence of the various coefficients. In Fig. 20 the results of the sensitivity analysis are shown for TC35, ZZ10 and ZZ20. As it can be noticed, the most important hull coefficients are, as expected,  $N_r$  and  $N_v$ ; this represents a crucial issue regarding the cancellation phenomenon, since main variations in manoeuvring behaviour of ship depend on these two coefficients, and they have an opposite effect on the manoeuvres; as a consequence, it is likely that they will tend to cancel with each other during identification loops.

In addition to the two linear coefficients  $N_r$  and  $N_v$ , rudder related coefficients, including the rudder lift slope coefficient and the two flow straightening coefficients, are also very important. In the present work, it was decided to include in the identification (at first step) only the flow straightening coefficient, since the rudder open water characteristics (in terms of the rudder lift slope) were considered reliable. Obviously, also the rudder related coefficients tend to cancel with the hull coefficients having similar effects.

Finally, the lateral force coefficients show a very limited effect with respect to yaw moment coefficients and rudder coefficients;

this results in a more difficult identification of these coefficients, since large variations are needed in order to obtain visible effects on the manoeuvres.

For the sake of completeness, the results of present analysis have been qualitatively compared with those presented in [44]. It is worth mentioning that the two analyses present some differences, since in [44] only linear hull derivatives were considered, together with rudder and propeller interaction parameters used in MMG model; in present case nonlinear hull derivatives were included in the analysis and, as mentioned before, the rudder force was considered by means of the lift slope curve.

Considering the similar parts, the majority of results are in agreement, since the  $N_r$  and  $N_v$  coefficients result very important in both cases. The interaction parameters have an important role too, and this is again similar, though in [44] the importance of the straightening coefficients was a bit lower. Acceleration derivatives appear to have low influence in both cases, even if  $N_{rr}$  appeared to be more influent (though still limited) in the present analysis for the ZigZag manoeuvre.

The main difference between the two analyses is represented by the  $Y_v$  coefficient, which in present case appeared of rather limited importance, contrarily to the results reported by Kose. A possible explanation of this could be the fact that in present case a rather slender hull form is considered, while in Kose interest was on full ships with high block coefficient.

Considering the present analysis of nonlinear derivatives, it allowed to show that they have a certain importance (still lower than the linear derivatives) on all manoeuvres and especially on those with larger rudder angle (as expected); moreover, it was shown that  $N_{rv}$  is the most influent parameter, followed by  $N_{rr}$ . Among the longitudinal force coefficients,  $X_{vr}$  showed some influence on turning circle manoeuvre, being responsible of the added resistance during turn.

## Appendix B. Identification 2 manoeuvring plots

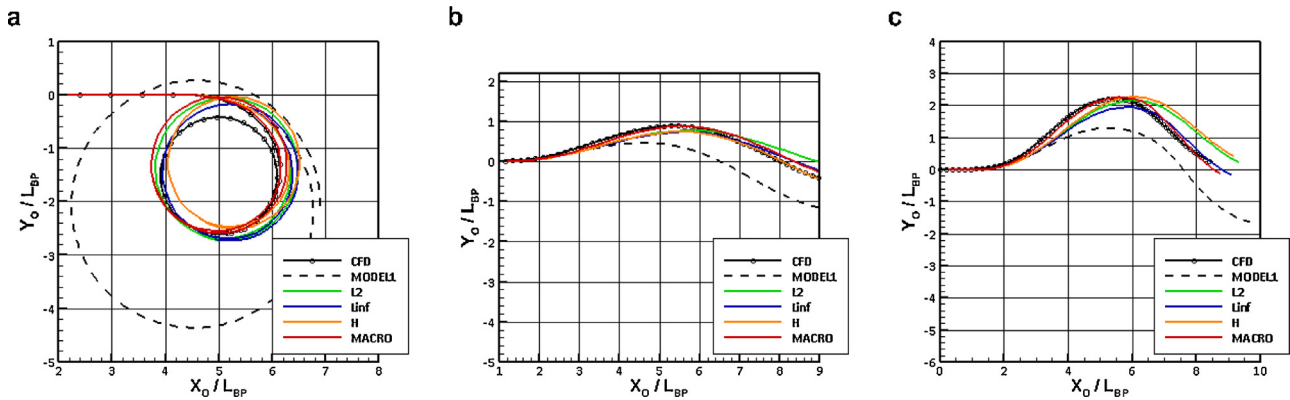


Fig. 21. ID2 trajectory of Turning Circle (a), ZigZag 10/10 (b), ZigZag 20/20 (c).

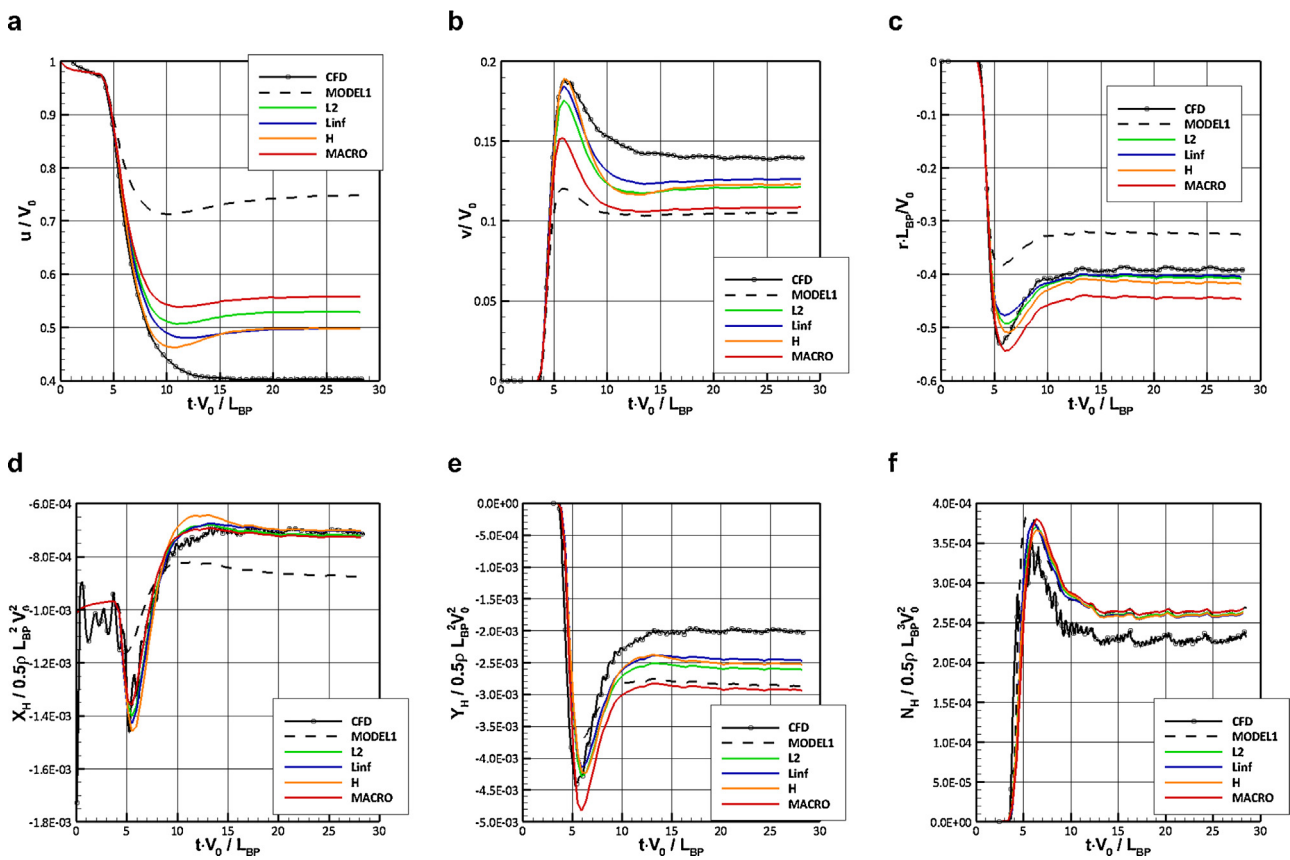


Fig. 22. Manoeuvring time histories of ID2 Turning circle; surge speed (a), sway speed (b), yaw rate (c), X hull force (d), Y hull force (e),  $N$  hull moment (f).

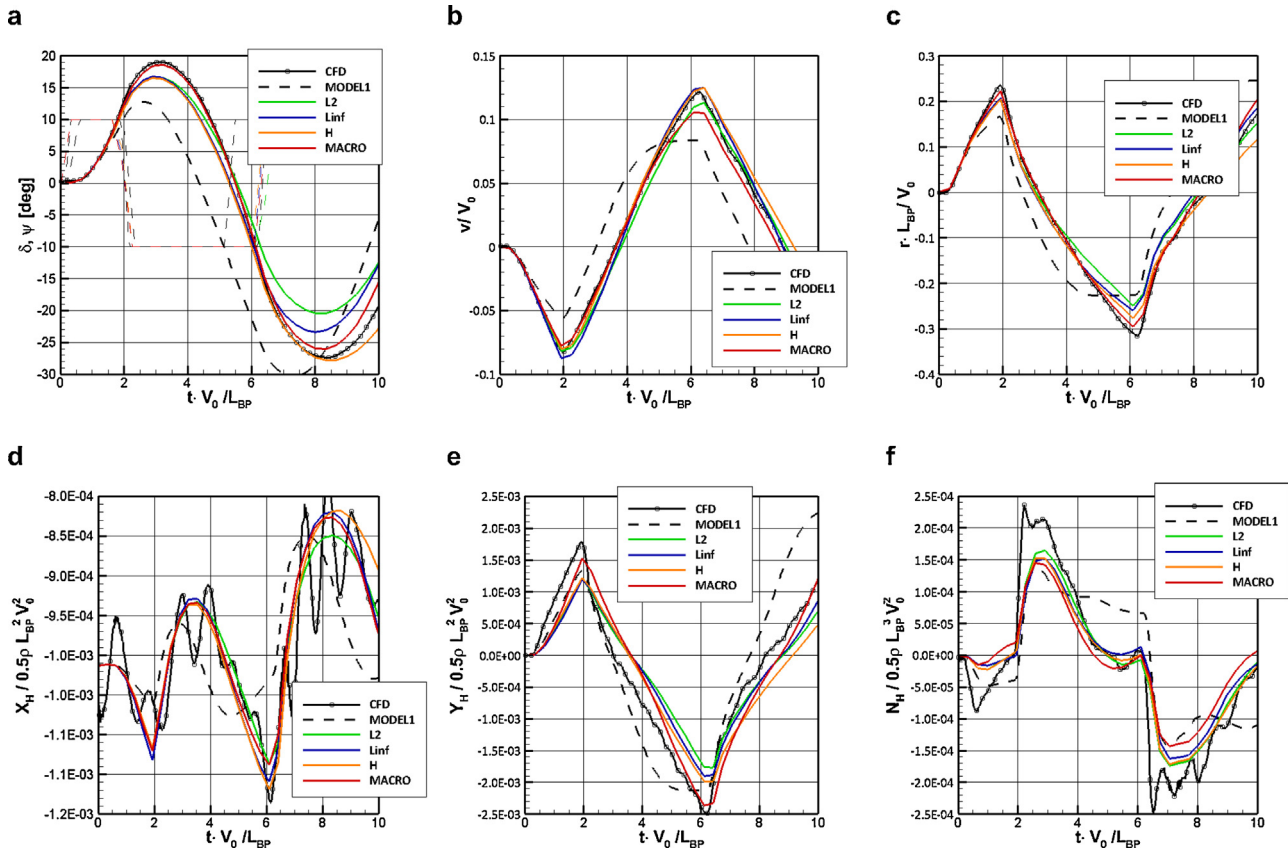


Fig. 23. Manoeuvring time histories of ID2 ZigZag 10/10; heading and rudder angles (a), sway speed (b), yaw rate (c), X hull force (d), Y hull force (e), N hull moment (f).

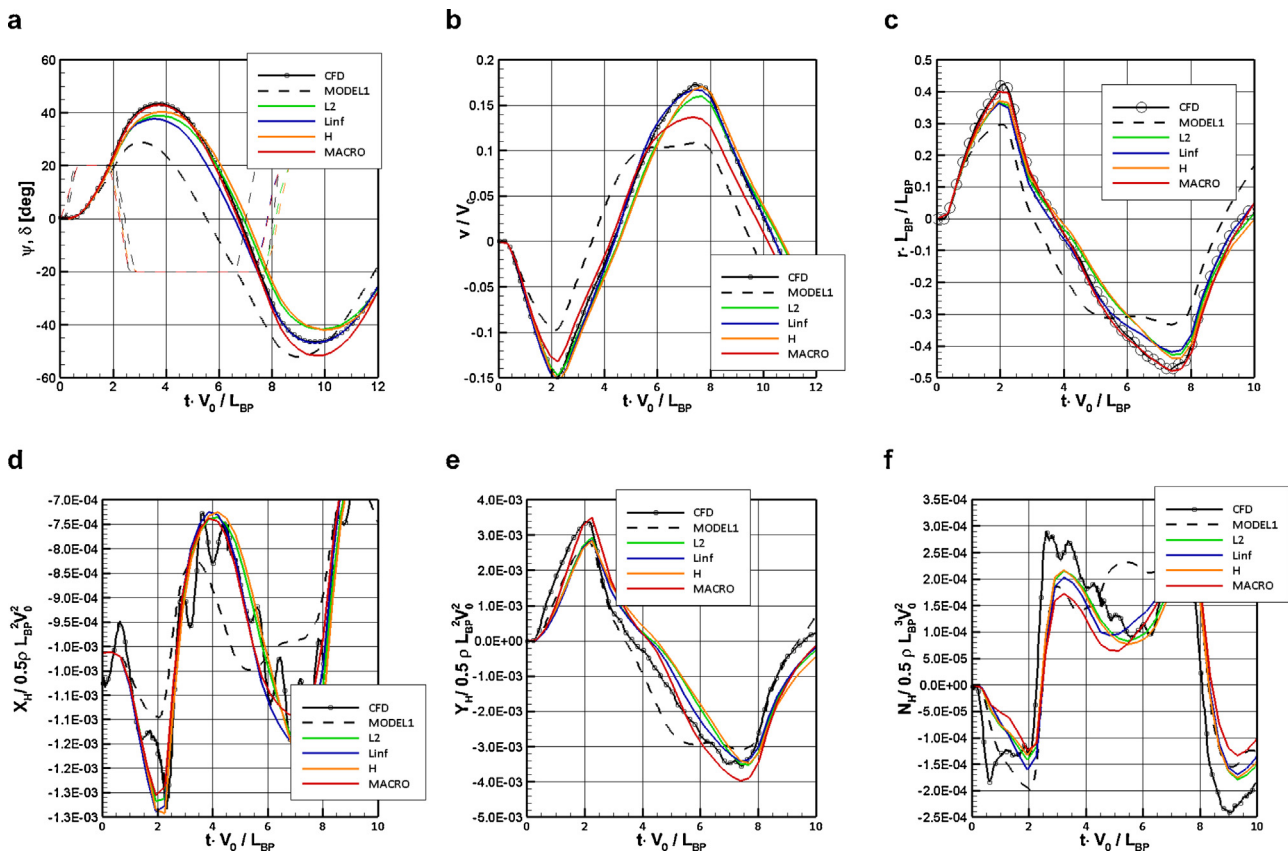


Fig. 24. Manoeuvring time histories of ID2 ZigZag 20/20; heading and rudder angles (a), sway speed (b), yaw rate (c), X hull force (d), Y hull force (e), N hull moment (f).

### Appendix C. Identification 3 and 4 manoeuvring plot

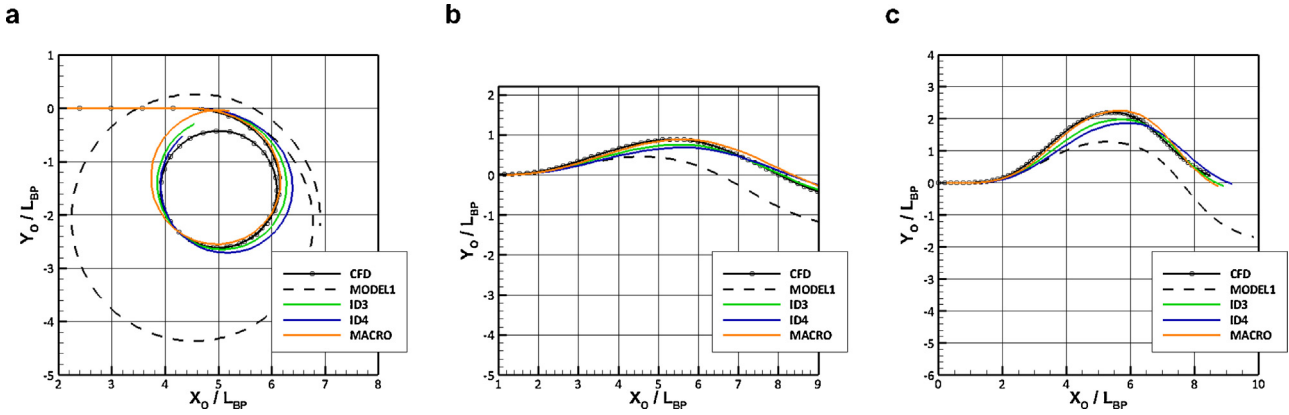


Fig. 25. Trajectory for Turning Circle (a), ZigZag 10/10 (b), ZigZag 20/20 (c).

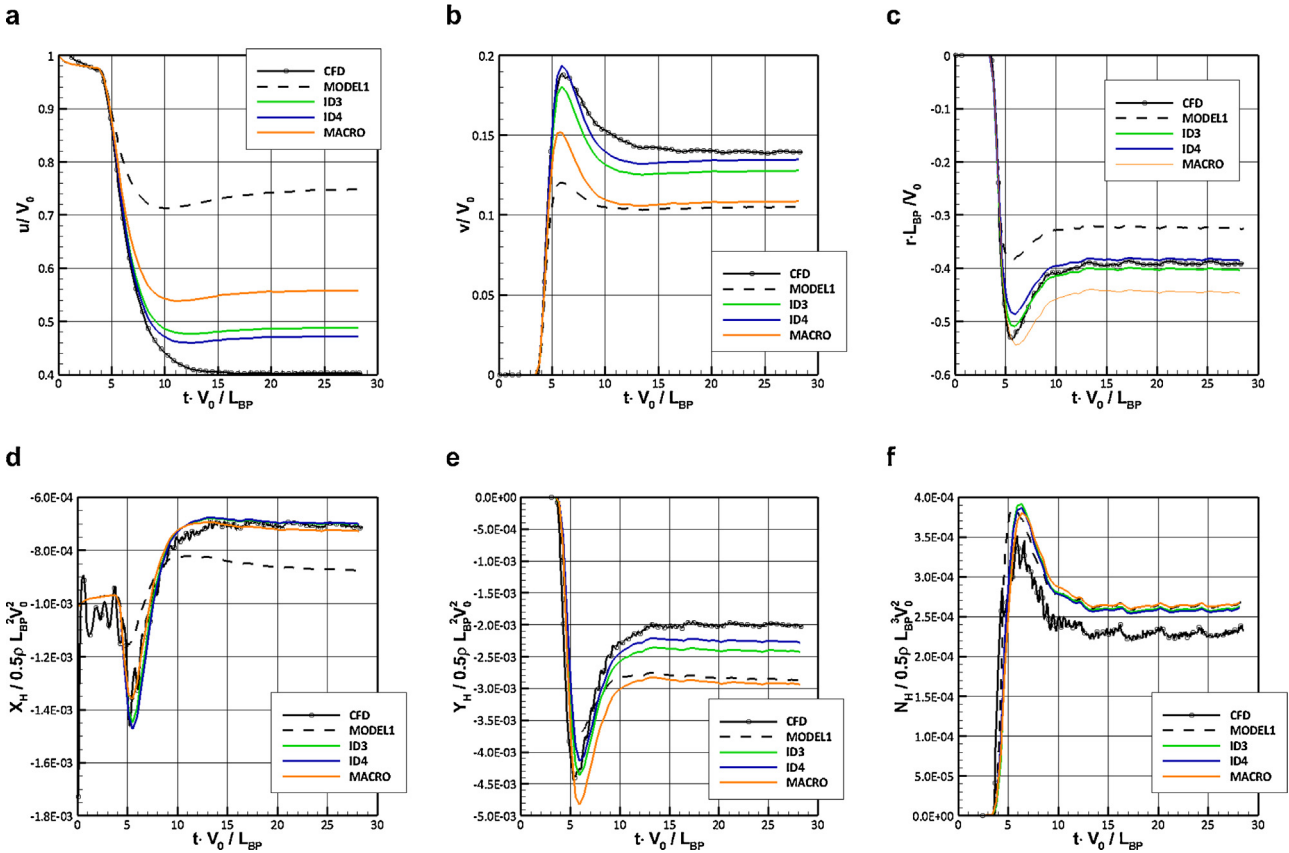


Fig. 26. Manoeuvring time histories of Turning circle; surge speed (a), sway speed (b), yaw rate (c), X hull force (d), Y hull force (e),  $N$  hull moment (f).

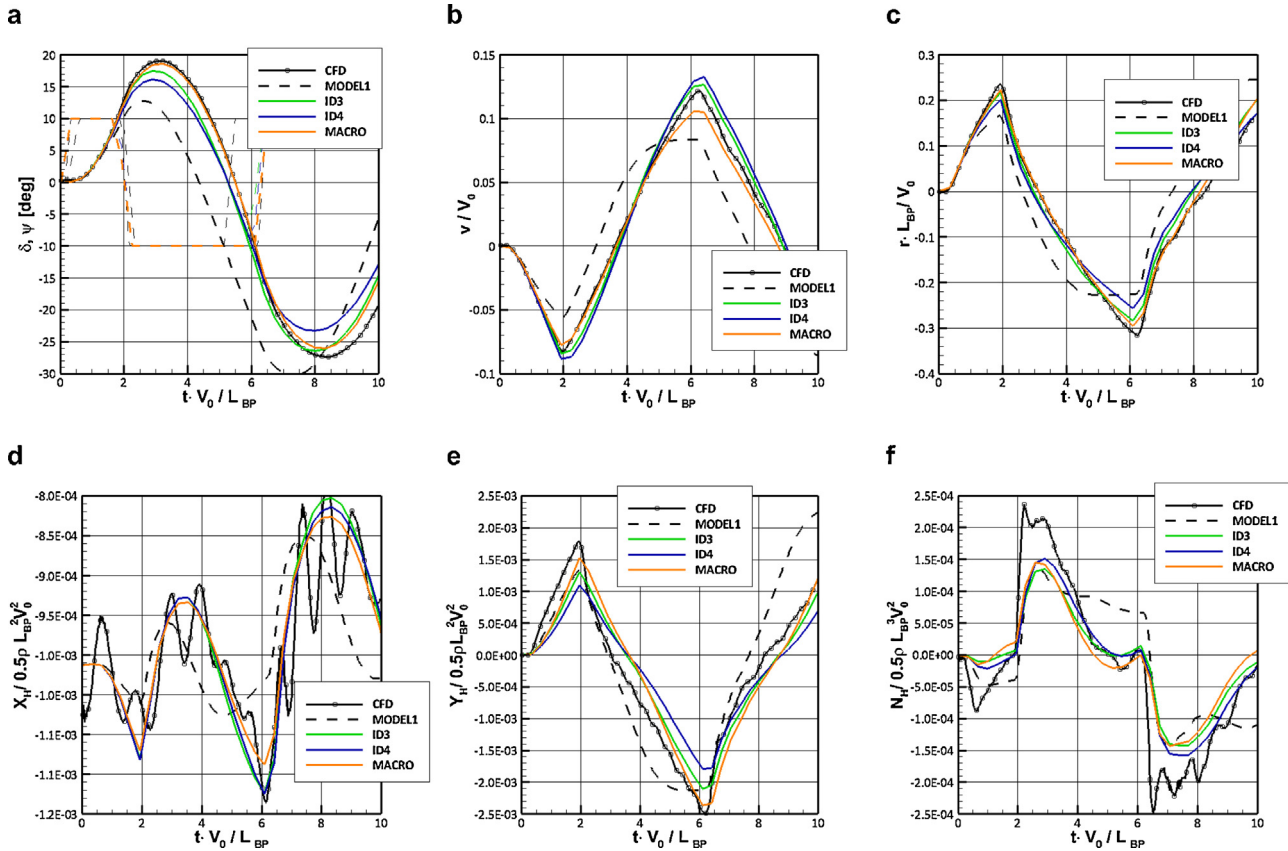


Fig. 27. Manoeuvring time histories of ZigZag 10/10; heading and rudder angles (a), sway speed (b), yaw rate (c), X hull force (d), Y hull force (e), N hull moment (f).

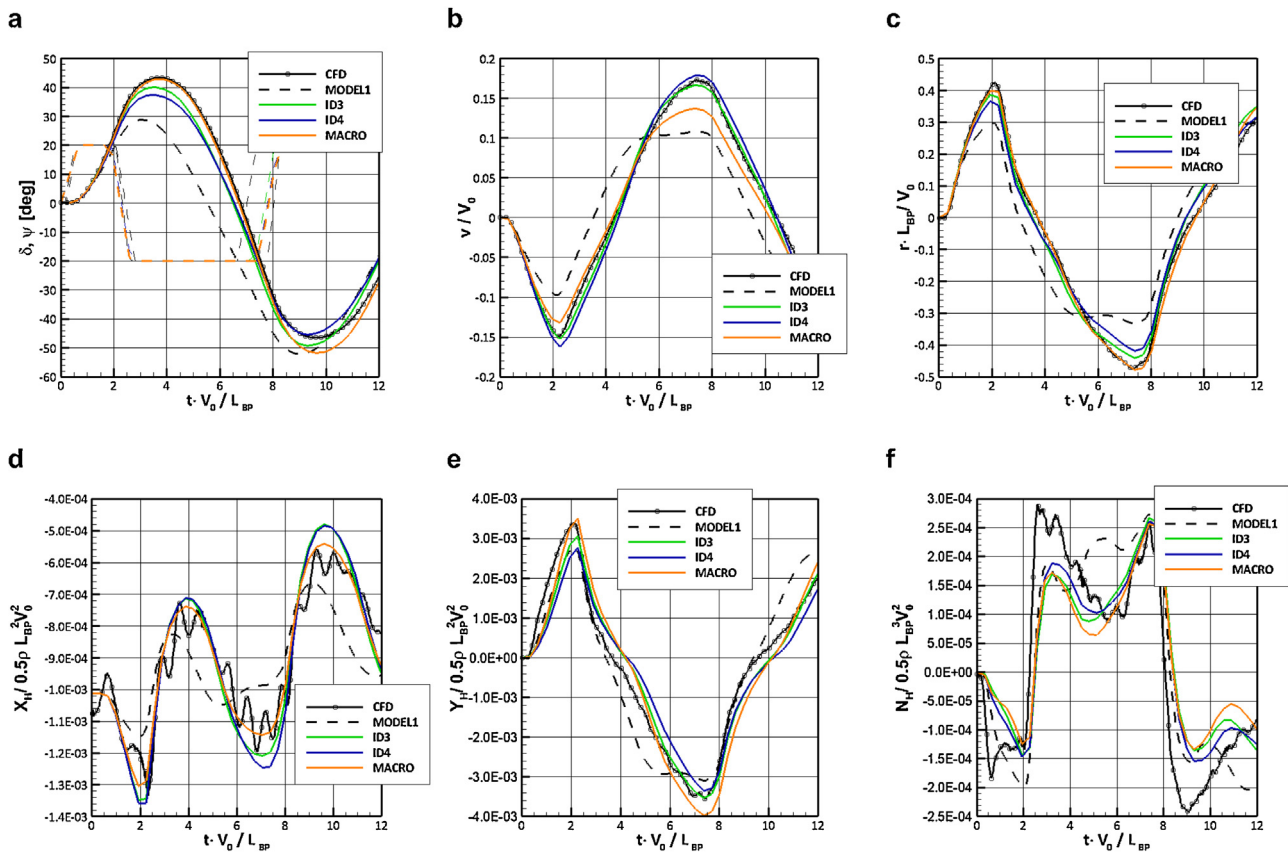


Fig. 28. Manoeuvring time histories of ZigZag 20/20; heading and rudder angles (a), sway speed (b), yaw rate (c), X hull force (d), Y hull force (e), N hull moment (f).

## References

- [1] Hwang W (Ph.D. thesis) Application of system identification to ship maneuvering. MIT; 1980.
- [2] Abkowitz MA. Measurement of hydrodynamic characteristics from ship manoeuvring trials by system identifications. SNAME Trans 1980;88.
- [3] Kallstrom CG, Astrom K. Experiences of system identification applied to ship steering. Automatica 1981;17:187–98.
- [4] Oltmann P. Roll – an often neglected method in ship manoeuvrability. In: Proc international conference on marine simulation and ship manoeuvrability (MARSIM), vol. II. New Foundland: St. John's; 1993. p. 463–71.
- [5] Rhee K, Kim K. A new sea trials method for estimating hydrodynamic derivatives. J Ship Ocean Technol (SOTECH) 2000;3(3):25–45.
- [6] Moelja A. System identification in ship maneuvering. Final project report. University of Twente – MARIN; 2001.
- [7] Yoon H, Rhee K. Identification of hydrodynamic coefficients in ship maneuvering equations of motion by Estimation Before Modeling technique. Ocean Eng 2003;30(18).
- [8] Bhattacharya S, Haddara R. Parametric identification for nonlinear ship maneuvering. J Ship Res 2006;50(3):197–207.
- [9] Luo W, Zou Z. Parametric identification of ship manoeuvring models by using support vector machines. J Ship Res 2009;53(1):19–30.
- [10] Wang X, Zou Z, Xu F, Ren RY. Sensitivity analysis and parametric identification for ship manoeuvring in 4 degrees of freedom. J Mar Sci Technol 2014;19(4):394–405.
- [11] Viviani M, Depascale R, Sebastiani L, Podenzana Bonvino C, Dattola R, Soave M. Alternative methods for the identification of hydrodynamic coefficients from standard manoeuvres. In: International conference on marine simulation and ship manoeuvrability (MARSIM). 2003. pp. RC-5.
- [12] Viviani M, Podenzana Bonvino C, Depascale R, Conti F, Soave M. Identification of hydrodynamic coefficients from standard manoeuvres for a series of twin screw ships. In: Proc 2nd international conference on marine research and transportation (ICMRT). 2007. p. 99–108.
- [13] Di Mascio A, Dubbioso G, Notaro C, Viviani M. Investigation of twin screw naval ships manoeuvrability behaviour. J Ship Res 2011;55(December (4)), <http://dx.doi.org/10.5957/JOSR.55.4.090031>, 221–248(28), ISSN: 0022-4502, Online ISSN: 1542-0604.
- [14] Proceedings of SIMMAN. Copenhagen: Force Technology; 2008.
- [15] Proceedings of SIMMAN. Lyngby: Force Technology; 2014.
- [16] Araki M, Sadat-Hosseini H, Sanada Y, Tanimoto K, Umeda N, Stern F. Estimating maneuvering coefficients using system identification methods with experimental, system-based, and CFD free-running trial data. Ocean Eng 2012;51:63–84.
- [17] Zilman G. Parameter identification of ships maneuvering (an ill-posed problem formulation). In: Proc 23<sup>rd</sup> American towing tank conference, 115. Washington: National Academy of Press; 1993. p. 17–24.
- [18] Favini B, Broglia R, Di Mascio A. Multigrid acceleration of second order ENO schemes from low subsonic to high supersonic flows. Int J Numer Methods Fluids 1996;23:589–606.
- [19] Di Mascio A, Broglia R, Favini B. A second order Godunov type scheme for naval hydrodynamics. Kluwer Academic/Plenum Publishers; 2001. p. 253–61.
- [20] Di Mascio A, Muscari R, Broglia R. An overlapping grids approach for moving bodies problems. In: 16th ISOPE. 2006.
- [21] Di Mascio A, Broglia R, Muscari R. On the application of the single-phase level set method to naval hydrodynamic flows. Comput Fluids 2007;36: 868–86.
- [22] Broglia R, Di Mascio A, Amati G. A parallel unsteady RANS code for the numerical simulations of free surface flows. In: Proc of 2nd international conference on marine research and transportation. 2007.
- [23] Spalart P, Allmaras S. A one-equation model for aerodynamic flows. La Research Aerospatiale 1994;1:5–21.
- [24] Zaghi S, Di Mascio A, Broglia R, Muscari R. Application of dynamic overlapping grids to the simulation of the flow around a fully-appended submarine. Math Comput Simul 2014, <http://dx.doi.org/10.1016/j.matcom.2014.11.00>.
- [25] Broglia R, Zaghi S, Muscari R, Salvadore F. Enabling hydrodynamics solver for efficient parallel simulations. In: Proc international conference on high performance computing & simulation (HPCS). 2014., <http://dx.doi.org/10.1109/HPCSim.2014.6903770>.
- [26] Hough G, Ordway D. The generalized actuator disk. Technical Report TARTR 6401, Therm Advanced Research, Inc; 1964.
- [27] Ribner H. Propeller in yaw. Langley Field: NACA Technical Report, Advanced Restricted report 3L09, Langley Memorial Aeronautical Laboratory; 1947.
- [28] Broglia R, Dubbioso G, Durante D, Di Mascio A. Simulation of turning circle by CFD: analysis of different propeller models and their effect on manoeuvring prediction. Appl Open Res 2013;39:1–10.
- [29] Dubbioso G, Durante D, Broglia R. ZigZag maneuver simulation by CFD for a tanker like vessel. In: MARINE 2013. 2013.
- [30] Broglia R, Dubbioso G. Prediction of the turning qualities characteristics of the KVLC2. In: Proceedings of SIMMAN 2014. 2014.
- [31] Dubbioso G, Durante D, Broglia R, Di Mascio A. Maneuvering prediction of a twin screw vessel with different stern appendages configuration. In: Proc of 29th ONR symposium on naval hydrodynamics. 2012.
- [32] Dubbioso G. Maneuverability behaviour of twin screw ships. PhD Thesis; 2011.
- [33] Dubbioso G, Viviani M. Aspects of twin screw ships semi-empirical manoeuvring models. Ocean Eng 2011;48(2012):69–80, <http://dx.doi.org/10.1016/j.oceaneng.2012.03.007>. ISSN 0029-8018 (Elsevier).
- [34] Ankudinov V, Kaplan P, Jacobsen BK. Assessment and principal structure of the modular mathematical model for ship manoeuvrability. In: Proc international conference on marine simulation and ship manoeuvrability (MARSIM). 1993.
- [35] Molland A, Turnock S. Marine rudders and control surfaces. UK: Butterworth Heinemann, Elsevier; 2006. ISBN 978-0-7506-944-3.
- [36] Bertram V. Practical ship hydrodynamics. Oxford, UK: Butterworth Heinemann; 2000.
- [37] Martelli M, Viviani M, Altosole M, Figari M, Vignolo S. Numerical modelling of propulsion, control and ship motions in 6 degrees of freedom. Proc Inst Mech Eng M: J Eng Maritime Environ 2014;373–97.
- [38] ModeFrontier4 Manual, ESTECO. (n.d.).
- [39] Cazzani G, Depascale R, Monaci F. Programma di Simulazione SIMSUP 5.1 – Manuale d'uso. Genova: CETENA; 2002.
- [40] Poles S. An improved multi-objective genetic algorithm. ESTECO Technical Report 2003-006; 2003.
- [41] Quagliarella D, Periaux J, Poloni C. Genetic algorithms and evolution strategies in engineering and computer science. England: John Wiley & Sons; 1997.
- [42] Broglia R, Dubbioso G, Di Mascio A. Prediction of manoeuvring properties for a tanker model by Computational Fluid Dynamics. In: AVT PANEL, Specialists meeting AVT-189/RSM-028 on "Assessment of stability and control prediction methods for NATO air and sea vehicles". 2011.
- [43] Sutulo S, Guedes Soares C. An algorithm for offline identification of ship manoeuvring mathematical models from free-running tests. Ocean Eng 2012;79:10–25.
- [44] Kose KA, Misiag W. A systematic procedure for predicting maneuvering performance. In: Proceedings of MARSIM'93 conference, 1. 1993. p. 331–40.